Faculdade de Engenharia da Universidade do Porto

FEUP

An endotelial cell-delivery system for therapeutic angiogenesis

Joana Bianchi Marques Bettencourt Gesta

Dissertação realizada no âmbito do
Mestrado Integrado em Bioengenharia
Major Engenharia Biomédica

Orientador: Dr. Cristina Barrias
Co-orientador: Dr. Sílvia Bidarra

20 de Setembro de 2013

Abstract

Neovascularization is a crucial step towards recovery of injured tissues. Since endothelial cells (ECs) are primary angiogenic cells, their delivery has been prominently studied as a pro-angiogenic strategy. Yet, up to now, clinical trials of ECs transplantation have not resulted in consistent benefits. The outcome might presumably be improved using biomaterial-based vehicles to protect cells from the harsh in vivo environment, enhancing their survival and engraftment. These carriers might also provide ECs with instructive signals to assist and promote their 3D organization, enhancing functional integration.

Alginate is an injectable polymer, widely used for cell entrapment, which is biologically inert but can be modified in order to stimulate specific cellular responses, namely through changes in its viscoelastic properties and/or grafting of bioactive peptides. In particular, previous studies showed that 3D culture in soft RGD-alginate hydrogels promote the self-assembly of entrapped cells, including ECs and mesenchymal stem cells (MSC), and the deposition of an endogenous fibronectin-rich extracellular matrix (ECM) by MSCs.

Therefore, the main aim of this work was to create an ideal microenvironment for EC entrapment using an integrative approach, combining this optimized hydrogel matrix with the use of co-entrapped MSCs as mural cells.

A variety of cell populations have been investigated in clinical revascularization trials. Here, the initial plan was to test two different cell types: human umbilical vein endothelial cells (HUVECs), a well-established model of mature ECs, and endothelial progenitor cells (EPCs) derived from human umbilical cord blood (UCB), which appear to have superior angiogenic properties than fully differentiated ECs such as HUVECs. UCB is a promising source of EPCs for therapeutic applications, as cells can be obtained through a non-invasive procedure, support long-term storage without losing biological properties, and have low immunogenicity, which makes them an interesting candidate for allogeneic transplantation. So, the first step was to isolate and characterize $CD34^+$ cells from UCB, and promote their differentiation into EPCs, which was performed using a previously published protocol. The isolated $CD34^+$ cells were able to form different hematopoietic colonies, in a standard methylcellulose assay, which confirmed their multipotency. The evaluation of phenotypic expression before and after a differentiation period of 21 days showed that differentiated $CD34^+$ cells expressed some EC-lineage markers like CD31, VE-cadherin, vWF and uptake of Ac-LDL and presented cluster formation with surrounding

spindle-shaped cells. Also, these cells were not able to form tube-like structures in Matrigel at any time-point. Overall, $CD34^+$ -derived cells phenotype resembled the so-called early EPCs.

Subsequently, soft RGD-alginate hydrogels were used as matrices for the 3D culture of ECs. HUVECs were cultured alone or in combination with MSCs, whose pro-angiogenic effects and pericyte-like roles have been widely reported. Cells viability and functionality were increased in co-cultured constructs, where the formation of multicellular structures, including EC cord-like structures, and deposition of endogenous ECM were also stimulated. When placed in a tissue mimic (Matrigel), co-cultures also promoted higher outward migration and cell sprouting. 3D cultures of $CD34^+$ cells in monoculture or co-cultured with MSC were also established. However, only freshly isolated $CD34^+$ cells were tested in a preliminary study, not only because it was important to assess how these cells behaved in soft-RGD alginate matrices, but also because the differentiation process was too lengthy to be implemented in 3D cultures in due time. Although $CD34^+$ cells did not perform well in 3D monocultures, interesting results were obtained when these were co-cultured with MSCs, and both cell types seemed to exert some influence over each other.
Finally, a preliminary characterization of the in vivo performance of cell-laden soft RGD-alginate hydrogels was carried out using the chorioallantic membrane (CAM) assay. Matrices were implanted immediately after preparation or following a pre-culture time of 5 days, and their angiogenic potential was evaluated. Although no significant differences were found between the different types of cultures (mono- vs. co-cultures), the pre-cultured matrices seemed to result in an increased stimulation of new vessels formation, suggesting that it might be advantageous to implant more mature cellular-ECM structures.

Resumo

Quando se pretende regenerar tecidos lesionados, a estimulação da neovascularização é um passo crucial. Tendo em conta que as principais células envolvidas no processo de angiogénese são células endoteliais (ECs), a transplantação das mesmas é uma das estratégias mais estudadas hoje em dia. Contudo, até hoje, os ensaios clínicos que envolveram o transplante de ECs não conseguiram assegurar os seus benefícios. Uma das maneiras de melhorar os resultados obtidos poderá ser, então, a utilização de biomateriais como veículos que protejam as células do ambiente hostil *in vivo* e permitam melhorar a sua sobrevivência e integração. Para além disso, estes veículos poderão ser modificados com sinais que orientem e suportem a sua organização em 3D, melhorando a integração do sistema.

O alginato é um polímero injetável natural muito usado para encapsular células. Este polímero é biologicamente inerte, podendo ser modificado de forma a estimular respostas celulares específicas e desejáveis através de ajustes nas suas capacidades viscoelásticas e/ou por adição de péptidos bioativos às suas cadeias. Mais especificamente, estudos recentes com células endoteliais e mesenquimais estaminais (MSCs) mostraram que culturas 3D em hidrogeis suaves de RGD-alginato promovem a reorganização das células e estimulam a deposição de uma matriz extracelular (ECM) endógena, rica em fibronectina, por MSCs.

Assim sendo, o principal objectivo deste trabalho seria o de criar o microambiente ideal para a encapsulação de ECs, combinando os conhecimentos relativos à matriz de hidrogel optimizada com o uso de MSCs como células murais.

Hoje em dia, já foram testados vários tipos de células em ensaios clínicos com vista a revascularização. Neste estudo, o plano inicial era o de testar dois tipos de células humanas: células endoteliais da veia do cordão umbilical (HUVECs) e células progenitoras endoteliais (EPCs) derivadas do sangue do cordão umbilical (UCB), sendo que a primeira população é correntemente usada como modelo de ECs maduras e a segunda, apesar de parecer possuir mais propriedades angiogénicas, ainda não se encontrar bem definida. O facto de as EPCs poderem ser isoladas de uma fonte rica em células progenitoras como UCB é uma grande vantagem pois permite a obtenção de células não imunogénicas por meios não invasivos. Para além disso, as EPCs podem ser armazenadas por longos períodos de tempo sem perder propriedades biológicas. Todos estes factores fazem destas células as candidatas ideais para transplantes alogénicos. Desta forma, o primeiro passo deste trabalho foi isolar, caracterizar as células $CD34^+$ presentes no UCB e promover a sua

diferenciação em EPCs segundo um protocolo previamente publicado. A análise do fenótipo exibido antes e depois de um período de diferenciação de 21 dias demonstrou que as células diferenciadas a partir de células $CD34^+$ exprimiram marcadores característicos de linhagens endoteliais como CD31, VE-caderina, vWF, incorporaram Ac-LDL e formaram agregados de células rodeados de células fusiformes. Para além disso, as células $CD34^+$ formaram colónias hematopoiéticas, e nem estas nem as células diferenciadas conseguiram formar estruturas tubulares em Matrigel. De uma maneira geral, as células derivadas de células $CD34^+$ apresentaram um fenótipo semelhante ao das EPCs precoces.

De seguida, hidrogeis moles de RGD-alginato foram usados como matrizes para a cultura 3D de ECs. HUVECs foram postas em cultura sozinhas ou em co-cultura com MSCs, cujos efeitos pro-angiogénicos e capacidade de atuar como pericitos foram vastamente reportados. A viabilidade e funcionalidade das células em co-cultura foram aumentados, da mesma maneira que foram estimuladas a formação de estruturas multicelulares tubulares, formadas por ECs, e deposição de ECM endógena. Quando estas matrizes foram colocadas em Matrigel, a co-cultura também promoveu maior migração para o exterior. Células $CD34^+$ foram também testadas em culturas 3D, sozinhas ou em co-cultura com MSCs. No entanto, só foram utilizadas células isoladas no momento, por ser importante analisar o seu comportamento nas matrizes utilizadas, mas também por o seu processo de diferenciação ser demasiado demorado para ser implementado em culturas 3D a tempo.

Apesar de o comportamento das células $CD34^+$ não ter sido satisfatório em monocultura 3D, foram obtidos resultados interessantes quando em co-cultura com MSCs, e ambos os tipos celulares pareceram exercer algum tipo de influência um sobre o outro.

Por fim, foi feita uma caracterização preliminar da performance dos hidrogeis moles de RGD-alginato com células embebidas *in vivo*, utilizando o ensaio na membrana corio-alântica de um embrião de galinha. As matrizes foram implantadas imediatamente após preparação ou após um período de pré-cultura de 5 dias, e o seu potencial de angiogénese foi avaliado. Apesar de não se terem detectado diferenças significativas entre os tipos de cultura (mono- e co-cultura), as matrizes previamente preparadas pareceram aumentar a estimulação da formação de novos vasos sanguíneos, indicando que talvez possa ser vantajosa a implantação de matrizes contendo estruturas de ECM mais maduras.

Acknowledgements

First of all, I'd like to thank Prof. Inês Gonçalves for helping me find a project of my interest and making the connections with the needed people. Likewise, I'd like to thank Prof. Mário Barbosa for giving me the opportunity to work at INEB.

Prof. Cristina, thank you for letting me in so "out of the blue" and trusting in my capabilities. Also, thank you for all the support, the insights and the help and, of course, the good humour that always made me feel welcomed.

Prof. Sílvia, thank you for all your help and your availability to answer my "doubts". Most of all, thank you for your patience!

David, thank you for introducing me around. Thank you for giving up your time to accompany me and sharing your knowledge.

Raquel Gonçalves, thank you for all your help with the flow citometry and methilcelulose, and for sharing your antibodies with me.

Raquel Maia, thank you for your help every time I needed, and of course for letting me use your alginate!

Filipa, thank you for the pleasant conversations outside, and for letting me drag you to the confocal microscope every time I could.

I'd also like to thank to Prof. Isabel Amaral and Estrela Neto, for kindly letting me borrow their antibodies, and Sara for helping me with the Live/Dead.

Last but not least, I'd like to thank all of the Biomatrix and INEB members (Daniela, Ana Luísa, Estrela, Filipa Lourenço, Ana Rita Ferreira, Tiago) for being so prompt to help and always having an encouraging (or funny!) thing to say.

Finally, I'd like to thank my family and friends for the support and comprehension, and especially to my mom, who always believes in me even when I don't.

Index:

List of figures:

List of tables:

List of abbreviations:

BM	Bone Marrow
BFU-E	Burst-forming Unit - Erithroyd
CAC	Circulating Angiogenic Cell
CCFM	Recovery Cell Culture Freezing Medium
CD	Cluster of Differentiation
CF	Colony-forming
CFU	Colony-forming Unit
CLSM	Confocal Laser Scanning Microscope
DMSO	Dimethyl Sulfoxide
EBM	Endothelial Basal Medium
ECFC	Endothelial Colony Forming Cell
ECM	Extracellular Matrix
ECGS	Endothelial Cell Growth Supplement
ECs	Endothelial Cells
EGF	Epidermal Growth Factor
EGM	Endothelial Growth Medium
EOC	Endothelial Outgrowth Cells
EPCs	Endothelial Progenitor Cells
EXP	Experiment
FBS	Fetal Bovine Serum
FGF	Fibroblast Growth Factor
FN	Fibronectin
GA	Gentamicin Amphotericin
GDL	Glucone Delta-Lactone
GEMM	Granulocyte, Eritrocyte, Monocyte, Megakaryocyte
GM	Granulocyte, Macrophage
HMW	High Molecular Weight
HSC	Hematopoietic Stem Cells
HUVECs	Human Umbilical Vein Endothelial Cells
IFM	Inverted Fluorescence Microscope
IGF	Insulin Growth Factor
IMDM	Iscoves Modified Dulbecco's Medium

LMW	Low Molecular Weight
MC	Mural Cells
MMP	Matrix Metalloproteinase
MNCs	Mononuclear Cells
MSCs	Human Mesenchymal Stem Cells
PFA	Paraformaldehyde
PI	Propidium Iodide
PBS	Phosphate Buffered Saline
Pen/Strep	Penicillin/Streptomycin
RGD	Arginylglycylaspartic acid
RT	Room Temperature
SD	Supplementary Data
TBS	Tris-Buffered Saline
UCB	Umbilical Cord Blood
VE-cad	Vascular Endothelial Cadherin
VEGF	Vascular Endothelial Growth Factor
vWF	Von Willebrand Factor

Introduction

1. DINAMICS OF NEOVASCULARISATION

Angiogenesis is the physiological process that leads to formation of new blood vessels from pre-existing vasculature in post-embryonic development. Blood vessels provide adequate oxygenation, nutrient delivery and removal of waste products in surrounding cells, as well as signaling molecules that might be involved in communication between organs. The importance of vascularization is based on the fact that diffusion between blood vessels and the surrounding cells is limited to a distance of up to 150-300 μm [1].

When new blood vessels are formed, it can happen either from the longitudinal splitting of an existing vessel – intussusceptive angiogenesis – or from the outgrowth of a new branch from preexisting blood vessels – sprouting angiogenesis. Yet, both of these processes occur via proliferation and migration of endothelial cells (ECs), which can be influenced by interaction with their extracellular matrix (ECM) [2] and involves the release of matrix metalloproteinases (MMP) by ECs to degrade the ECM [3]. Communication between ECs, between ECs and other cells and between cells and ECM is vital throughout the entire process.

Vasculogenesis is other type of neovascularization that happens more frequently in embryonic development (although reports have been made of its occurrence in adult life [4]), and consists in the de novo formation of blood vessels from angioblasts: endothelial progenitor cells form blood islands that fuse and sprout, forming a primary plexus that later expands via angiogenesis and vasculogenesis [5]. In this case, endothelial progenitor cells (EPCs) are mobilized to sites of neovascularization and differentiate into ECs in situ – see **Figure 1**.

Mature endothelial vessels are formed by an endothelial layer that is stabilized by mural cells (which depend on the size of tube: pericytes in cappilaries and vascular smooth muscle cells in more complex vessels) and a basement membrane that embeds them [6].

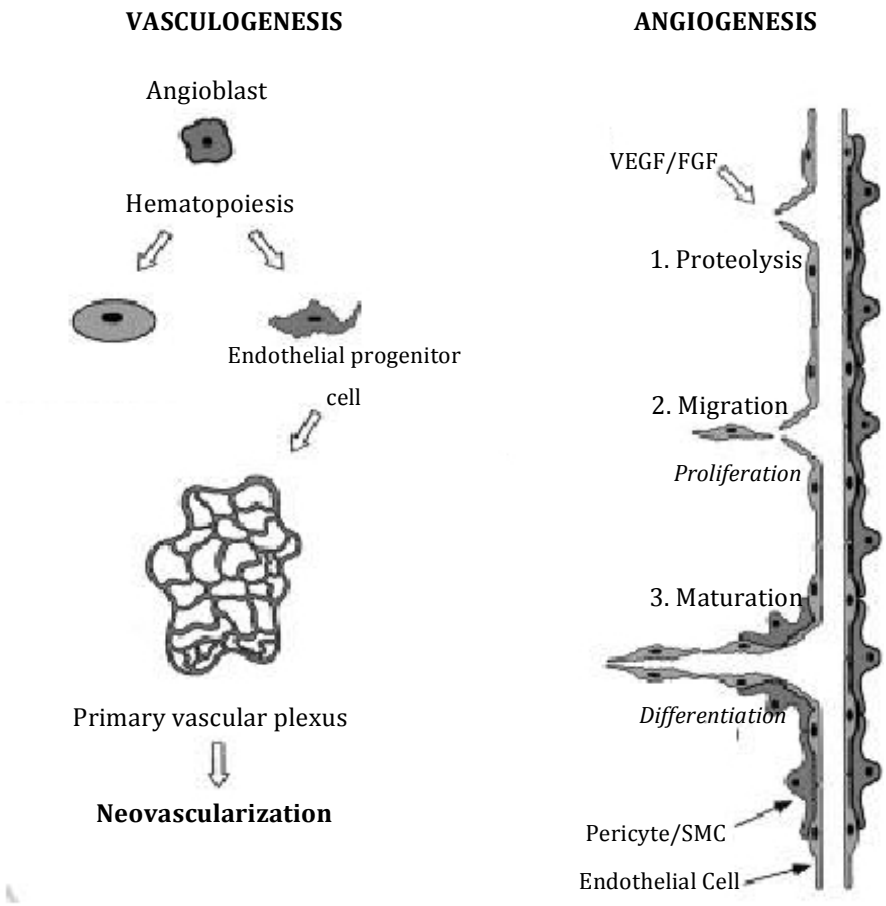

Figure 1 – Overview of the neovascularization processes and the main steps it involves. *(GERWINS, P. ET AL.)*

2. NEOVASCULARISATION AS A TISSUE REGENERATION STRATEGY

The main goal of tissue engineering strategies is to repair damaged, injured or missing body tissues in a way that its functions maintain assured. Engineered tissues of a clinically relevant size and complexity must have their own vasculature or easily develop it after implantation, allowing rapid and stable perfusion so that the area and its surrounding tissue is repopulated, preventing cell death and tissue necrosis. Many approaches have been devised in order to improve angiogenesis and vasculogenesis in bioengineered tissues for later implantation, taking into consideration the knowledge on phisiological mechanisms of neovascularisation.

Implants can present neovascularization that results from either the invasion of host blood vessels and/or neovascularization *in vivo*, or from the prevascularization *in vitro* or *in vivo* before implantation [6]. **Figure 2** depicts the main cell-based approaches to promote neovascularization of a bioengineered tissue. Also, Novosel et al. published a review that delves into these subjects [1]. Prevascularization is of great importance in

thick constructs, since it accelerates functional anastomosis, through connection with the host existing vasculature upon implantation. Prevascularization can be stimulated by cell seeding and neovascularization stimulation *in vitro* (**Figure 7-A**) [7], or by implantation of unseeded scaffolds into a host body (**Figure 7-B**). Host blood vessels penetrate the scaffold, building a perfusable vascular network, and these scaffolds are then explanted and reimplanted into the ischemic target site [1].

Anyhow, neovascularization *in vitro* or *in vivo*, can be achieved by seeding relevant cell types in the target area. Endothelial cells (ECs) compose the inner lining of blood vessels, and secrete several paracrine factors (such as growth factors) that are known to be involved in the stimulation of angiogenesis – hence, these are the most comon "single-cell-type" cultures used for angiogenesis stimulation assays [8]. However, it is known that ECs and their progenitors (EPCs) are not the only cells involved in neovascularization and that more cell types are found in mature blood vessels, leading to the use of more than one cell type in these assays (**Figure 7-E**).

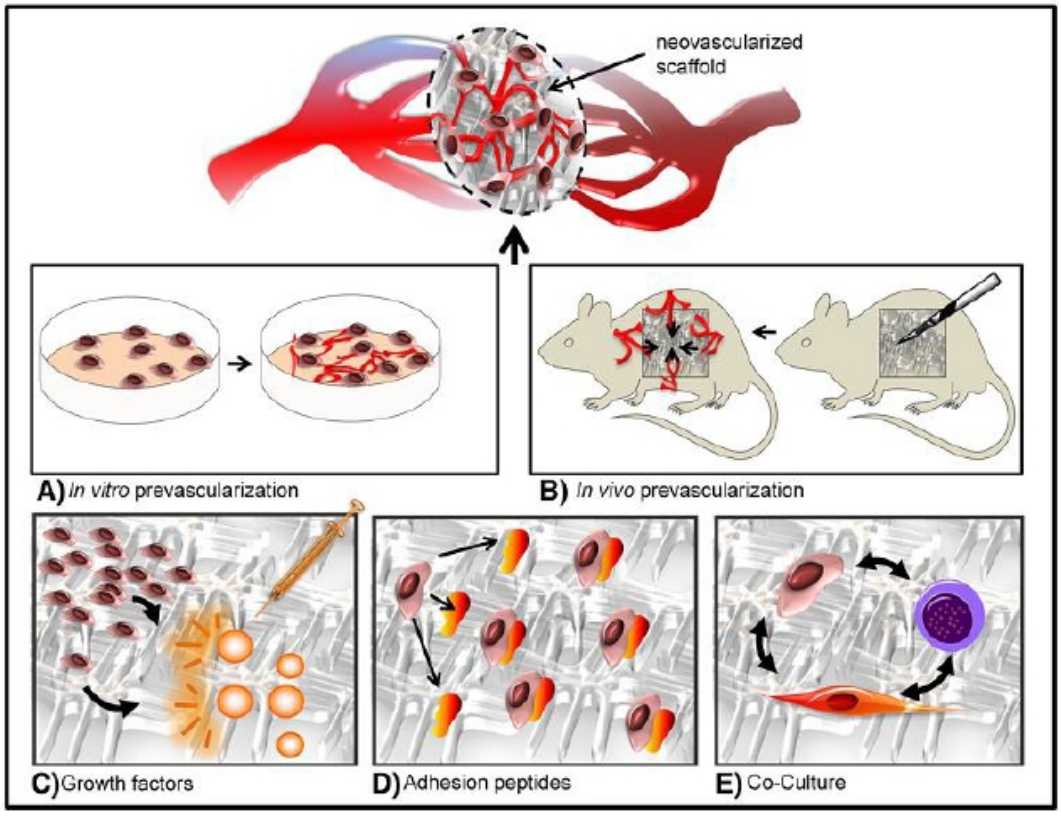

Figure 2 – Different approaches for cell-based neovascularisation enhancement in bioengineered tissues. The bioengineered tissues can be prevascularized either *in vitro (A)* or *in vivo (B)*, through their implantation into host bodies and then removal and reimplantation into the target ischemic tissue. Also, the constructs can release growth factors (C) or be grafted with adhesion peptides like RGD sequences (D). Finally, these constructs can contain more than one type of cells that are involved in neovascularization (E). *NOVOSEL, E.C. ET AL.*

The ECM that surrounds blood vessels consists mostly of hydrated proteins and proteoglycans, yet is responsible for mechanical and biochemical stimuli that regulate cell behavior [9]. The influence of grafted growth factors (**Figure 7-C**) and adhesion peptides (**Figure 7-D**) that stimulate scaffold-cells interaction on angiogenesis is a major subject currently under study, in order to fully understand and ultimately mimic the normal biological processes occurring inside the body during neovascularization [6].

3. ENDOTHELIAL CELL DELIVERY TOWARDS NEOVASCULARISATION STIMULATION

3.1. MATURE ENDOTHELIAL CELLS FOR NEOVASCULARISATION

For neovascularisation in cell delivery therapies, ECs are one of the primary types of cells to be seeded. Mature endothelial cells have limited regenerative capacity, since they are fully differentiated, and their phenotype is slightly different in every source. Still, they can be isolated from many parts of the human body, such as the umbilical vein (HUVECs), dermal microvasculature (HDMECs) and vasculature in general (HVECs), and are easy to identify. Mature endothelial cells preferentially express some genes and molecular markers: expression of CD31, CD34, von Willebrand factor (vWF) and dil-acetylated low density lipoprotein (Ac-LDL) uptake are the most common markers when distinguishing ECs from other cells in culture using flow cytometry or immunohistochemistry. Other relevant markers used to discriminate mature ECs during differentiation are E-selectins, VE-cadherin (vascular endothelial cadherin) and N-cadherin: these molecules are involved in cell adhesion between ECs or between ECs and other cells present in angiogenesis like pericytes, fibroblasts and smooth muscle cells (SMCs) [10]. Previous studies from our group where HUVECs were used have shown that these cells can proliferate, reorganize into cellular networks and even migrate when they were encapsulated into alginate [11].

A comon disadvantage of mature endothelial cells is that, in order to prevent an immune reaction, the patient's own cells would have to be collected from a blood vessel, a process that can cause morbidity at the donor site, and they also present low proliferation rates and low availability. As a result of these impairments, the scientific community's attention has been turning to endothelial progenitor cells (EPCs), a heterogeneous minor subpopulation of blood mononuclear cells (MNCs) that play a significant role in postnatal vasculogenesis [1]. EPCs are believed to be mobilized to damaged tissues in case an emergent vascular regenerative process is happening, and represent an advantageous cell type for cell delivery therapies, since blood can be collected from the patient and these

cells can be isolated and expanded in vitro [12]; this way, the implant will stimulate tissue regeneration without causing an immune response. They also present aditional advantages, as detailed below.

3.2. ENDOTHELIAL PROGENITOR CELLS

Since Asahara et al. [13] originally reported the isolation of EPCs, efforts have been made to characterize each type of cells comprised under the term "EPCs". However, there is not a standardized isolation and culture protocol being used yet. Asahara's group claims that there are two main types of EPCs, acording to their origin: hematopoietic lineage EPCs and nonhematopoietic lineage EPCs [14]. "Hematopoietic EPCs" represent a heterogeneous subpopulation of hematopoietic stem cells (HSCs) with provasculogenic characteristics. These EPCs can be isolated from bone marrow (BM) or blood and include colony-forming EPCs (CF-EPCs), non-colony forming "differentianting" EPCs or even adherent circulating angiogenic cells (CACs), among others. "Nonhematopoietic EPCs" are adhesive angiogenic and vasculogenic cells that present mature EC-like phenotypes or differentiate into it., yet do not form hematopoietic colonies in methylcelulose. Nonhematopoietic EPCs can be isolated from blood or tissue samples; however, these cells primary origin is still unknown. Endothelial outgrowth cells (EOC) are the main member of this group of EPCs. **Figure 3** describes the general EPC dynamics: although all of the EPCs seem to be responsive to stimulation that causes them to migrate to damaged tissues, the role they play in tissue regeneration is different.

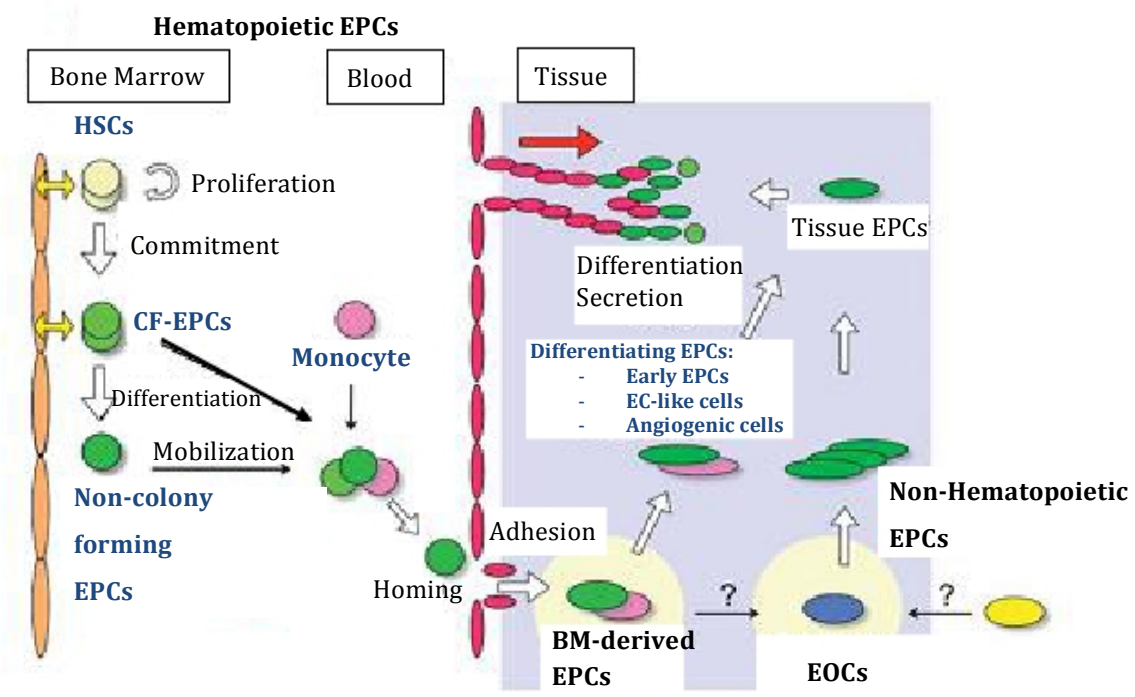

Figure 3 – Putative circulating EPCs dynamics. *Adapted from Asahara, T. et al.*

On the other hand, Prater's group has categorized EPCs regarding their phenotype: early EPCs and late EPCs [15]. Accordingly to this classification, CF-EPCs and CACs constitute early EPCs, since they appear in culture after 4-9 days. Early EPCs have angiogenic and vasculogenic potential, are capable of vascular integration and express EC markers, but do not form tube-like structures or present a cobblestone-like morphology when in culture [14]-[16]. Endothelial colony forming cells (ECFCs) are classified as late EPCs, since they take about 7 to 21 days to be detected in culture [17]. These EPCs form tube-like structures in culture and present a phenotype that is similar to mature endothelial lineage [15], [18]. **Figure 4** presents common methods of EPC culture, their morphology and the main groups that characterized each type of cells.

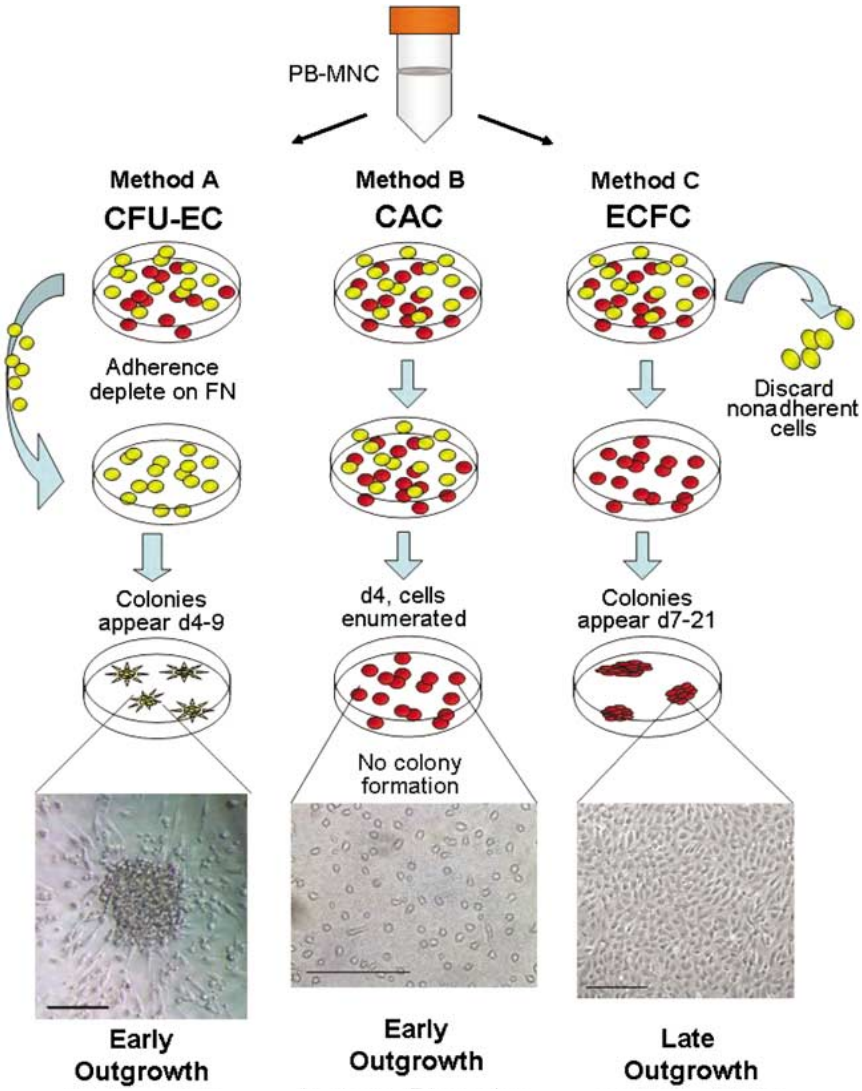

Figure 4 – Common methods of EPCs isolation and culture. Method A: CFU-ECs are obtained after a culture period of 5-days, where non-adherent MNCs differentiate into adherent EPC colonies. Scale bar = 100 μm. Method B: Circulating angiogenic cells appear after 4-7 days in culture, and typically do not form CAC cultures. Scale bar = 200 μm. Method C: ECFCs derive from adherent MNCs and are detected after 7 to 21 days in culture. These cells usually display a cobblestone-like appearance. *Scale bar = 400 μm. Yellow: non-adherent cells; Red: adherent cells.*

Recently, several groups have been focusing in $CD34^+$-selected populations, isolated from MNCs, as an EPC-enriched fraction. Even though this marker is also expressed on hematopoietic stem and progenitor cells, this fraction has been yielding positive results regarding neovascularisation stimulation and angiogenesis potential [19], [20]. However, $CD34^+$ cells still form a heterogeneous population [21], and their differentiation and phenotype varies according to their culturing method [22].

CD34+-derived EPCs have the advantage of being isolated through non-invasive means [23] and having great expansion potential. However, not only their expansion and maintenance is more successful when they are co-cultured with mesenchymal stem or progenitor cells (MSCs) [24], their viability and angiogenic behavior has already been proven to be increased when they are co-cultured with many types of cells, like MSCs [25], $CD34^-$ cells [26] and even $CD34^+$-derived ECs [20].

3.3. CO-CULTURE: THE SUPPORTING ROLE OF MESENCHYMAL STEM CELLS

So far, bone marrow-derived and cord blood-derived MSCs were proven to be able to act as pericytes (perivascular cells), providing paracrine signals that stimulate ECs to form tubular structures, and promote and stabilize newly forming structures in vitro and in vivo [23], [27]. The stimulation MSC-derived perivascular cells confer to the growing blood vessels is attained by secretion of pro-angiogenic cytokines and regulation of cell-cell adherens junctions, which leads to regulation of the vessels permeability and perfusion and makes them less susceptible to regression. Also, our group has already shown that MSCs can self-assemble and produce ECM within RGD-grafted alginate [28], as well as promote multicellular networks formation by HUVECs when encapsulated in alginate microspheres [11]. Another advantage of MSCs is that their isolation does not yield donor site morbidity, allowing us to use the patient's own cells and prevent an immune response.

3.4. CELL DELIVERY VEHICLES

Many research groups have tried to mimic the ECM *in vitro*, not only using naturally derived biomaterials but also synthetic biomaterials with some type of modification; however, there are many factors and limitations that have to be controlled [9]. In order to mimic vascularisation in engineered tissues and/or deliver vascular cells, a suitable extracellular environment should also be developed. Therefore, scaffolds should ideally

promote cell survival, allow cellular reorganization, and allow cell-driven remodeling processes.

Hydrogels can be formed from several natural and synthetic materials, mostly under mild conditions. Also, they are easily modified and highly permeable to oxygen and water-soluble molecules. From the range of possibilities within hydrogels, natural hydrogels have the advantage of innately exhibiting some of the properties that characterize soft tissues [29].

Alginate is one of the most widely used hydrogels: it is a polysaccharide, derived from brown algae, which can crosslink *in situ* in the presence of divalent cations (e.g. Ca^{2+}), with low toxicity, and therefore can be injected into the target site, what makes it a minimally invasive therapy. Thanks to the alginate's versatility, its non-fouling characteristics and non-adhesiveness to cells can be overcome by covalently modifying it with cell-adhesion peptides (namely, containing the arginine-glycine-aspartic acid aminoacid sequence – RDG). This strategy has already been studied in previous works within our group [11], [30], [31]. Besides that, it is also possible to adjust its mechanical properties through molecular weight distribution and partial oxidation, and their degradation rate can be regulated using crosslinking peptides that are susceptible to cleavage by MMPs [32]. Regarding injectable pro-angiogenic therapies, these hydrogels have been most commonly tested as growth-factor delivery (usually VEGF) vehicles [33], [34]. In order to validate these hydrogels as endothelial cell celivery vehicles and their pro-angiogenic properties, *in vitro* and *in vivo* studies have to be performed.

4. PRELIMINARY *IN VIVO* ASSESSMENT OF PROANGIOGENIC PROPERTIES

In vitro assays have the advantage of being easy to interpret and involving well-controlled conditions, what facilitates the assessment of angiogenic effects [35]. However, *in vivo* studies have to be performed in order to analyze the host's response and the pro-angiogenic properties of endothelial cell delivery vehicles.

The simplest and most extensively used *in vivo* assay is performed in the chorioallantoic membrane (CAM) of a chick embryo. The CAM is an extra-embryonic membrane with an extensive vascular network that grows rapidly and lines the inner shell membrane, being so thin that becomes almost transparent and planar. To implant scaffolds onto the CAM, a window is opened in the shell, exposing the CAM and allowing the placement of the scaffold **(Figure 4)**. Afterwards, this window can be closed with transparent tape or a glass slide to prevent dehydration [36], and the grafts can be recovered after an appropriate length of incubation time. Therefore, this assay provides an

easy way to directly assess and quantify the formation of blood vessels using stereo-microscopy; also, the embryo's inflamatory reaction to the implant and morphology of the newly formed vessels can be assessed by immunocytochemistry. Finally, fertilized specific pathogen-free (SPF) chicken eggs are relatively cheap and easy to obtain, which makes the CAM assay a lot more appealing [37].

For all of the above reasons, the CAM assay is the best stepping stone between *in vitro* 3D studies and more detailed *in vivo* studies with a mammalian model.

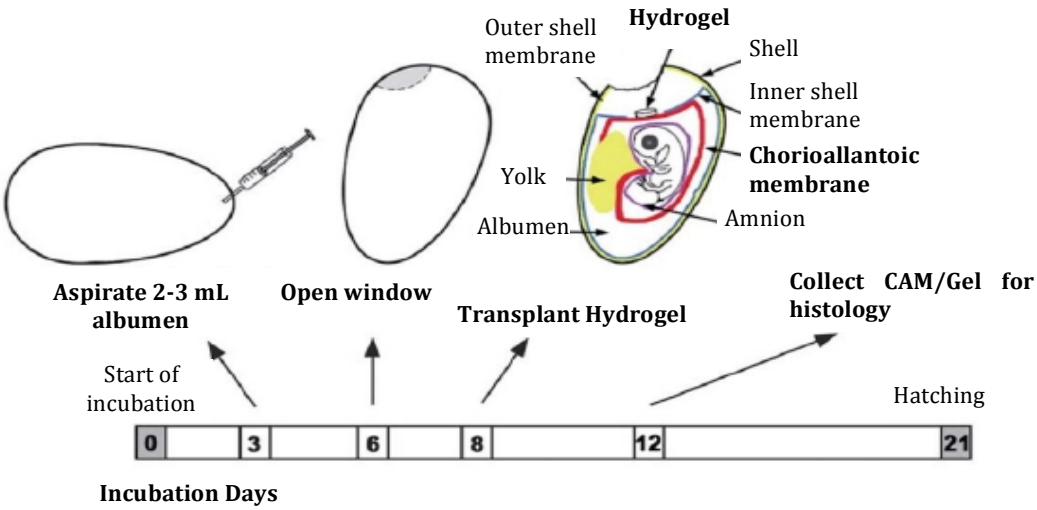

Figure 5 – Representative time-dependent diagram of the *in vivo* CAM assay. The transplantation and collection of the hydrogel can be made at different times, as long as one does not get too close to the hatching date. *(LIU, XI et al.)*

Material And Methods

1. ISOLATION AND CHARACTERIZATION OF CD34$^+$ CELLS

1.1. ISOLATION OF MNCS FROM UCB

Umbilical cord blood samples were collected during labor at Hospital S. João. All of the donors signed an informed consent form that is in compliance with the Portuguese legislation and the ethical committee of the referred hospital approved the collection. After collection, the samples were stored and transported in 250 mL sterile bags that contained 35 mL of CPDA-1 (Citrate, Phosphate, Dextrose and Adenine) anti-coagulant solution. Mononuclear cells were isolated from blood using Ficoll (Histopaque-1077 Hybri Max; Sigma-Aldrich, St. Louis, USA) density gradient separation **(see Figure S-1, in Supplementary Data – SD)**. MNCs rings were pipetted onto 50 mL Falcon tubes, washed with twice their volume of IMDM (Iscoves Modified Dulbecco's Medium; Invitrogen, Carlsbad, USA) and afterwards resuspended in CCFM (Recovery Cell Culture Freezing Medium; Invitrogen) at a density of about 10^8 cells/mL. Samples were frozen and stored at -80ºC.

1.2. ISOLATION OF CD34$^+$ CELLS FROM MNCS

MNCs were defrosted and the freezing medium was neutralized in 10% v/v FBS-enriched (Fetal Bovine Serum; Invitrogen) IMDM. Cells were resuspended in MACS buffer (PBS; 0.5% w/v BSA, Sigma-Aldrich; 2mM EDTA, VWR, Pennsylvania, USA) at a density of 1 x 10^8 cells/300 µL and marked using a CD34 MicroBead Kit (Myltenyi Biotec, Bergisch Gladbach, Germany). Succinctly, MNCs were incubated for 30 min at 4ºC with magnetic CD34 microbeads (microbeads conjugated to monoclonal mouse anti-human CD34) and FcR blocking reagent (human IgG) to prevent non-specific binding, using 100 µL of each solution for every 10^8 cells. After being washed with MACS buffer, the labeled cells were positively selected for CD34 expression using the mini-MACS immunomagnetic separation system (Myltenyi Biotec). The suspension was filtered through a 30-mm nylon mesh and loaded onto a column within a magnetic field. CD34$^+$ cells (bound to the CD34 microbeads) were eluted after the column was removed from the magnet. The resulting cell solution was loaded onto a new column and the purification step was repeated. The final cell solution was submitted to several characterization assays: assessment of expression of EC markers using fluorescence-activated cell sorting (FACS), detection and characterization of colony formation in methylcellulose and *in vitro* cell culturing towards ECs differentiation.

1.3. FLUORESCENCE-ACTIVATED CELL SORTING ANALYSIS

$CD34^+$ cells suspension and suspensions of $CD34^-$ cells (which resulted from negative selection in the first and second columns) were aliquoted (1.25-2.0 x 10^5 cells per condition), centrifuged and resuspended in FACS Buffer (PBS; 0.5% w/v BSA; 0.01% w/v Azide, Sigma-Aldrich). Half of each suspension was incubated for 30 minutes at 4ºC with isotype controls (Mouse IgG1 FITC and Mouse IgG1 R-PE; Caltag Medsystems, Buckingham, UK) or antigen-specific mouse anti-human antibodies: CD31-APC (Myltenyi Biotec), CD34-FITC and CD38-PE (both from Caltag Medsystems). In the first assays, dead cells were marked with PI (Propidium Iodide Staining Solution; BD Biosciences, USA, www.bdbiosciences.com) before washing with FACS buffer. However, after identifying this population in the FACS results, cell suspensions were just washed and fixed with 1% w/v paraformaldehyde (PFA; Merck Millipore, Darmstadt, Germany). Markers expression analysis was carried out by three-color flow cytometry on a FACSCalibur flow cytometer (BD Biosciences). Data analysis was made using FlowJo software. At least three experiments were tested for each sample.

1.4. METHYLCELLULOSE ASSAY FOR COLONY CHARACTERIZATION

$CD34^+$ cells were resuspended in complete endothelial growth medium (EGM) and 50 ng/mL of VEGF – endothelial basal medium (EBM™-2; Lonza, Gaithersburg, Maryland, USA); SingleQuots® growth factors (EGM™-2 SingleQuots; Lonza): Hydrocortisone, hFGF-B, VEGF, IGF-1, Ascorbic acid, hEGF, GA-1000 and Heparin; 20% v/v FBS (Invitrogen); and 1% v/v Penicillin/Streptomycin (Pen/Strep; PAA, New Jersey, USA). 1 x 10^4 cells were aliquoted from the cell suspension, mixed with methylcellulose-based semi-solid culture medium (MethoCult®H4230; StemCell Technologies Inc., London, UK) and distributed among 3 wells of a 4-well plate. The 4^{th} well of each plate was filled with PBS to prevent dehydration and the plates were incubated for 14 days at 37ºC in a humidified atmosphere with 5% v/v CO_2 in air. Three types of colonies were identified and counted after the incubation period: CFU-GM; BFU-E, CFU-GEMM.

1.5. DIFFERENTIATION OF $CD34^+$ CELLS INTO ECS

Isolated $CD34^+$ cells were resuspended in EGM with 50 ng/mL of vascular endothelial growth factor (VEGF; Sigma-Aldrich) and plated onto 1% w/v gelatin-coated 48-well plates, at a density of approximately 1 x 10^5 cells/well. Starting on the 5^{th} day of culture, every 2 days half of the medium was replaced and fresh VEGF was added. The cells were incubated for 21 days at 37ºC in a humidified atmosphere with 5% v/v CO_2 in air. The

expression of EC markers and functionality and behavior of the cells were assessed after 5 and 21 days.

1.6. DETECTION OF EXPRESSION OF EC MARKERS

Immunofluorescence staining was performed to assess the expression of EC markers. $CD34^+$ cells were fixed with 4% v/v PFA for 30 minutes at room temperature, washed with PBS and permeabilized with 0.2% v/v Triton X-100 (Sigma-Aldrich) in PBS for 10 minutes. To maintain the cadherin's morphology, the respective samples were incubated for 10 minutes in ammonium chloride (50 mM NH_4Cl, Sigma-Aldrich) before permeabilization. After washing with PBS, the samples were incubated for 1 hour at room temperature in blocking solution (4% v/v FBS in 1% w/v BSA in PBS) and incubated overnight at 4ºC with the following primary anti-human antibodies: monoclonal mouse CD31 (PECAM1; Dako, Denmark) and VE-cadherin (VE-cad; Santa Cruz Biotechnology, Texas, USA) and polyclonal rabbit von Willebrand factor (vWF; Dako). Excess antibody was removed by washing with PBS and the secondary antibodies (AlexaFluor® 594 anti-mouse and anti-rabbit; both from Invitrogen) were incubated for 1 hour at room temperature. The nucleus of cells was stained with FluoroShield™ containing 4',6-diamidino-2-phenylindole (FluoroShield™ with DAPI; Sigma-Aldrich). In each experiment, HUVECs (Passage 6-8) were used as a positive control, and HUVECs without any primary antibody staining were used as a negative control to validate the assay. Samples were visualized under a Zeiss inverted fluorescence microscope (IFM; Zeiss Axiovert 200, Carl Zeiss International, Germany, www.zeiss.com) and the resulting images were processed using Fiji Imaging Software.

1.7. ASSESSMENT OF PHENOTYPE EXPRESSION

Samples were incubated with 10 µg/mL of DiI-labeled acetylated low-density lipoprotein (DiI-Ac-LDL; Biomedical Technologies, Stoughton, USA) for 2 hours at 37ºC and washed three times with EGM. The uptake of Ac-LDL was visualized under an inverted fluorescence microscope.

1.8. IN VITRO TUBE FORMATION ON MATRIGEL PLATE

$CD34^+$ cells in culture were trypsinized and resuspended at a concentration of 6×10^4 cells/mL of EGM. One well of a 24-well cell suspension plate was coated with 0.3 mL of Matrigel™ (BD Biosciences) and incubated for 30 minutes at 37 ºC. 1 mL of cell suspension was seeded on top of the Matrigel and the plate was incubated for 24 hours at 37ºC in a humidified atmosphere with 5% v/v CO_2 in air. Cord formation was evaluated by phase

contrast microscopy on a Zeiss microscope (IFM). HUVECs (Passage 10) were used as a positive control.

2. *IN VITRO* STUDIES WITH 3D CULTURES

2.1. CELL CULTURE CONDITIONS

HUVECs and MSCs (Lonza) were routinely kept in culture at 37ºC in a humidified atmosphere with 5% v/v CO_2 in air. Media was changed every two days: HUVECs were cultured in complete M199 (Sigma-Aldrich) with 10% v/v FBS, 0.1 mg/mL Heparin (Heparin Sodium Salt; Sigma-Aldrich), 1% v/v Pen/Strep. Endothelial Cell Growth Supplement (ECGS; BD Biosciences) at a concentration of 3 µL/mL was added every time the media was changed. MSCs were cultured in Dulbecco's Modified Eagle medium (D-MEM; Invitrogen) with 10% FBS and 1% P/S. Both HUVECs and MSCs were trypsinized when they reached confluence. For the following experiments, cells from passages 6 and 7 were used. Regarding $CD34^+$ cells, isolation was made according to the method described in **Section 1.2** and there was no incubation period prior to cell embedment. In co-cultures, either HUVECs or $CD34^+$ cells in suspension were mixed (1:1 ratio) with MSCs. In all 3D conditions, cells were maintained in EGM during the culturing period.

2.2. CELL INCORPORATION WITHIN RGD-GRAFTED ALGINATE HYDROGEL MATRICES

To achieve RGD-grafted alginate hydrogel disks at a final concentration of 1 wt.% in polymer and 100 µM of RGD, a gel precursor solution of previously prepared and modified alginates (according to Bidarra's protocol [31]) was prepared at a concentration of 2 wt.% in polymer and 200 µM of RGD. To do so, high molecular weight (HMW) oxidized alginate with and without grafted RGD were mixed (6.9 mg and 8.1 mg, respectively) with 15 mg of low molecular weight (LMW, 15 mg) oxidized alginate and dissolved in 0.9 wt.% sodium chloride (NaCl; Sigma-Aldrich). The final alginate solution was filter-sterilized (0.22 µm filters) before use. The hydrogel's concentration and composition was chosen so that entrapped cells could adhere to the hydrogel and still have the necessary mobility to rearrange and, when needed, migrate, as reported by Fonseca et al. [32] and Bidarra et al. [31].

Three types of culture were tested in each 3D experiment: a co-culture of HUVECs or $CD34^+$ cells with MSCs (1:1 ratio) and monocultures of each cell type alone (HUVECs or $CD34^+$ cells and MSCs). In each condition, each type of cells was entrapped at a density of approximately 5 x 10^6 cells/mL – therefore, the disks seeded with cells in co-culture had a

cellular density of approximately 10 x 10^6 cells/mL. MSCs suspended in serum-free DMEM were labeled with CellTracker™ Blue (Invitrogen) by incubation with 15 µL of the stock solution (prepared according to the manufacturer) during 30 minutes and then with complete DMEM for another 30 minutes.

The alginate gel precursor solution and cells were aliquoted for each condition and the preparation of the disks was carried out in the following way (gently homogenizing the mixture at every step): the RGD-alginate gel precursor was mixed with fresh solutions of calcium carbonate ($CaCO_3$; Sigma-Aldrich) and filter-sterilized glucone delta-lactone (GDL; Sigma-Aldrich), both dissolved in NaCl, to trigger gelification. The $CaCO_3$/GDL molar ratio was set at 0.125, which leads to initial acidification of the medium but prevents deposition and crystallization of $CaCO_3$ [32]. This mixture was then combined with one of the aliquoted cell suspensions (HUVECs or $CD34^+$ cells, MSCs, HUVECs in co-culture with MSCs or $CD34^+$ cells in co-culture with MSCs, all of them previously centrifuged and resuspended in NaCl) and 17 µL of the final mixture were pipetted into each well of a 24-well cell suspension plate. The cell-laden hydrogel matrices were left to crosslink for 1 hour at 37ºC before EGM was added. The medium was changed 30 minutes after (since it becomes acidic during gelification) and the constructs were incubated at 37ºC in a humidified atmosphere with 5% v/v CO_2. Every condition had at least 3 replicates.

2.3. CHARACTERIZATION OF CELL CULTURES WITHIN ALGINATE DISKS

Regarding cell culture within alginate disks, all three conditions were tested throughout 3 days and at 3 time-points (2h, 24h and 72h). Two experiments were performed: one with HUVECs and one with $CD34^+$ cells. Characterization was made according to: metabolic activity, cell viability, uptake of Ac-LDL and expression of actin and fibronectin. At every time point, photographs of the disks were taken using a stereoscopic microscope (Olympus SZX10).

2.4. METABOLIC ACTIVITY AND CELL VIABILITY

The metabolic activity of entrapped cells in alginate matrices was measured 2, 24 and 72 hours after encapsulation for HUVECs/MSCs and 24 and 72 hours for CD34+/MSCs. Resazurin (Resazurin Sodium Salt at 0.1 mg/mL; Sigma-Aldrich) was diluted (20% v/v) in EGM and incubated with the disks for 2 hours at 37ºC. A fluorometer (Synergy MX; Biotek, Winooski, US) was used to excite the samples at 530 nm and read the fluorescence at 590 nm. EGM with resazurin was used as a blank sample.

Cell viability within alginate disks was determined with a Live/Dead assay. The disks were washed twice in Phenol Red-free IMDM (IMDM, no Phenol Red; Invitrogen) and

incubated for 45 minutes at room temperature (RT) with working solutions of 2 μg/mL calcein AM and 2.5μg/mL ethidium homodimer (both from Invitrogen). Afterwards, the constructs were washed twice with Phenol Red-free IMDM and visualized under a laser-scanning microscope (CLSM, Leica TCS-SP2 AOBS; Leica Microsystems, Wetzlar, Germany). The resulting images were processed using Fiji Imaging Software.

2.5. CELL MORPHOLOGY AND FIBRONECTIN EXPRESSION

Incorporation of DiI-Ac-LDL was used as a cell marker for HUVECs and an indicator of phenotype differences in $CD34^+$ cells, (as described in **Section 1.7**.); The disks were fixed in 4% PFA in TBS/$CaCl_2$ before visualization, and the 24 and 72 hours constructs were also incubated with phalloidin (Alexa Fluor®-488 Phalloidin; Invitrogen) for 1 hour, to label F-actin filaments.

Extracellular fibronectin was stained at 24h and 72h. 3D constructs were fixed with 4% v/v PFA in TBS/$CaCl_2$ for 30 minutes at room temperature, washed with TBS/$CaCl_2$ and permeabilized with 0.2% v/v Triton X-100 (Sigma-Aldrich) in TBS/$CaCl_2$ for 10 minutes. The samples were then incubated for 20 minutes at room temperature in blocking solution (1% w/v BSA in TBS/$CaCl_2$) and left overnight at 4ºC with mouse anti-human fibronectin monoclonal antibody (DSHB, Yowa, USA). Excess antibody was removed by washing with TBS/$CaCl_2$. The secondary antibody (AlexaFluor® 594 anti-mouse) and phalloidin were incubated for 1 hour at room temperature. Samples were visualized under a CLSM and the resulting images were handled using Fiji Imaging Software.

2.6. *IN VITRO* MIGRATION ASSAY OF 3D CULTURE

HUVECs were incubated with 15 μL/mL of CellTracker™ Green (Invitrogen) in serum free M199 and washed with complete M199; MSCs were labeled with CellTracker™ Blue, using IMDM, as previously described**.** HUVECs/MSCs-laden soft RGD-alginate hydrogel disks were prepared as described in **Section 2.2.**; After the first crosslinking hour, 2-chamber slides Lab-Teks® (Electron Microscopy Sciences, Hatfield, US) were filled with Matrigel™ (150-200 μL/cm^2) and the cell-laden constructs were loaded onto the chambers 5 minutes after gelification had started (as represented in **Figure S-2, SD)**. After 30 minutes at 37ºC, EGM was added to all chambers and the Lab-Teks® were incubated for 48h at 37ºC in a humidified atmosphere with 5% v/v CO_2. Every condition had at least 3 replicates.

Phase-contrast micrographs were taken in an IFM after 2, 24 and 48 hours of incubation. Data was analyzed using Fiji Imaging Software.

3. *IN VIVO* STUDIES WITH 3D CULTURES

3.1. MATRICES IMPLANTATION

Soft RGD-alginate hydrogel disks containing HUVECs and MSCs in mono and co-culture (1:1) with no cellular staining were prepared as described in **Section 2.2**. Two experiments with mono- and co-cultures were performed: one in which the disks were kept in culture for 5 days before testing, and another where the disks were placed on the CAM on the same day they were prepared. Each disc was implanted onto the CAM of 10 days-old chick embryos and an O-ring (5 mm diameter) was put on top of it to prevent the disks from getting lost.. EBM was added at the time of incubation and every day for 3 days to prevent dehydration.

After 3 days, the embryos were fixed with 4% w/v PFA in TBS/$CaCl_2$. The CAM area surrounding the O-ring was cut out and photographed using a stereoscopic microscope (Leica M205). The newly formed vessels around the constructs were counted from the CAM fragment and the average and standard deviation of each condition was calculated. The CAMs were then kept in PBS for further histological analysis.

4. STATISTICAL ANALYSIS

When applicable, data was analyzed by t-tests and Turkey's multiple comparison tests and results were considered statistically different at $p<0.05$. Prism™ Software was used to perform statistical analysis.

Isolation and characterization of $CD34^{+}$ Cells

AIM

The first experiments were performed in order to optimize the isolation of CD34+ cells from umbilical cord blood (UCB). UCB-derived CD34+ cells were isolated from several donors and the isolated populations were characterized by flow cytometry. Also, the expression of different endothelial and progenitor cell markers was assessed before and after differentiation.

Ultimately, the objective of this work was to obtain and characterize EPCs from a CD34-enriched population, following a previously established protocol, where the isolation of CD34+ cells from MNCs was reported to yield late EPCs.

RESULTS

1. ISOLATION OF CD34+ CELLS

The process of CD34+ cells isolation was repeated using 10 different UCB samples from different donors. The overall efficiency of the isolation protocol was represented by the average number of cells obtained after each of its key steps: isolation of mononuclear cells (MNCs), defrosting MNCs (which are frozen after isolation), isolation of CD34+ cells from MNCs and viability of CD34+ cells measured by flow cytometry. The detailed values for each experiment are available in **Supplementary Data (SD)**, **Figure S-1**. The number of cells considerably decreased from step to step (**Figure 6)**, as the simple process of

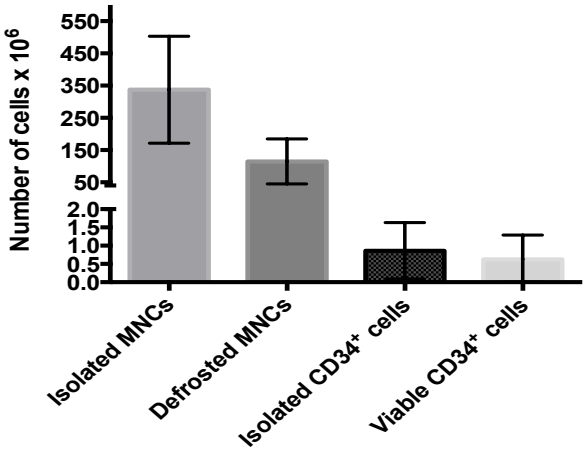

Figure 6 – Efficiency of CD34+ cells isolation. The first column represents the average amount of MNCs isolated from UCB (n=10); the second one, the average number of viable MNCs after freezing and defrosting the previous MNCs (n=10); the third column depicts the average number of CD34+ cells isolated from each sample of UCB (n=10); and the last column represents the number of viable cells in each CD34+ cell suspension (measured by FACS, n=4).

freezing and thawing isolated MNCs led to a loss of around 36 ± 15% of the cells. Within each sample of MNCs, only 0.66±0.32% was obtained after magnetic cell sorting for CD34 marker; furthermore, according to flow cytometry results, 69±21% of these cells was viable.

2. CHARACTERIZATION OF $CD34^+$ CELLS

After magnetic cell sorting, three samples were aliquoted from each experiment: the negatively selected cell suspension from the first column (Negative 1), the negatively selected cell suspension from the second column (Negative 2), and the positively selected cells from the second column (Positive). Flow citometry analysis was performed using cells suspensions from four different experiments. In **Table I,** expression of CD31, CD34 and CD38 markers in percentage of live population is presented; each sample's gated population and correlation scatters are presented in **Figure 7**. Dead cells and cellular debris were excluded from the gated population by comparison with preliminary results in which cell suspensions were marked with PI – representative scatters are available in **SD, Figure S-4**; also, the expression of these markers by isotypes can be consulted in **SD, Figure S-5**.

FACS analysis showed that the isolation of $CD34^+$ cells was successful, with 84.97±14.97% of the cells in the Positive sample expressing CD34. Also, these cells had higher expression of CD31 (97.81±1.72%). In fact, most of the $CD34^+$ cells in the positive samples were also CD31+, according to the percentage of $CD34^+CD31^+$ cells (91.23±8.63%). Likewise, the percentage of CD34+CD38- cells was higher in the Positive sample (19.58±18.98%). Neither Negative 1 nor Negative 2 samples had high expression of CD34, as expected, but they had high CD31 expression. Accordingly to these data, the cell population in the Positive samples will be referred to as "$CD34^+$ cells" from now on, and the Negative 2 samples will be termed "$CD34^-$ cells".

Table II – FACS analysis of CD34, CD31 and CD38 expression. Negative 1 and Negative 2 are the negatively selected cell suspensions from the first and second MACS columns, respectively. Positive is the positively selected cell suspension from the second column – CD34 marked cells. *The displayed values are averages of four experiments (n=4). Detailed values for each experiment are available in SD – Table S-I.*

	% CD34+ cells	% CD31+ cells	% CD34+CD38- cells	% CD34+CD31+ cells
Negative 1	0.46 ± 0.49	78.24 ± 10.23	0.00	16.46 ± 8.03
Negative 2	8.68± 9.98	82.24 ± 4.88	0.81 ± 0.93	25.68 ± 12.36
Positive	84.97 ±14.79	97.81 ± 1.72	19.58 ± 18.98	91.23 ± 8.63

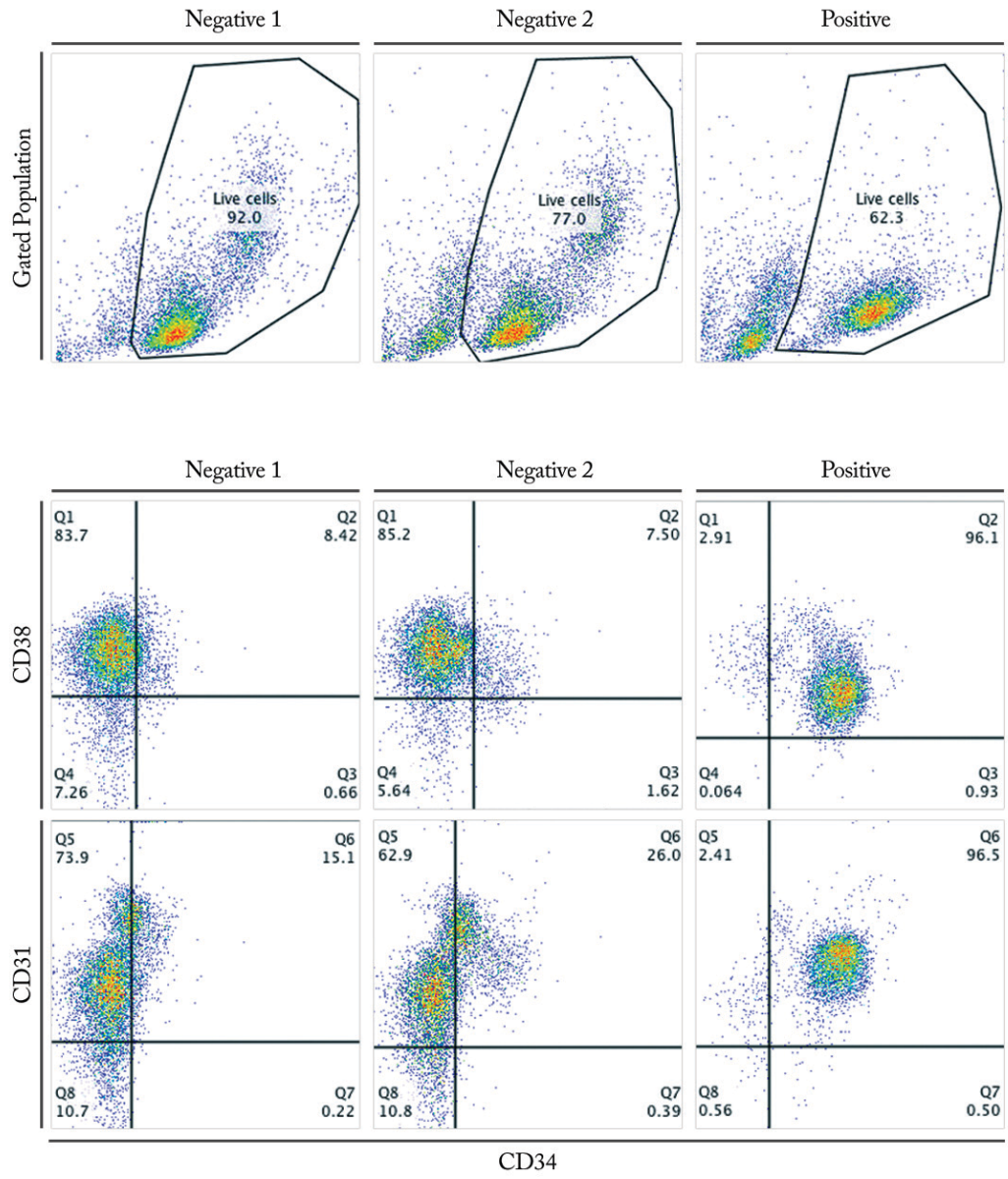

Figure 7 – FACS analysis scatter images. The first three images represent each sample's gated population (FSC-H vs. SSC-H). The second row scatters correlate the expression of CD34 (FL1-H) and CD38 (FL2-H) and the scatters in the last row correlate CD34 expression with CD31 expression (FL4-H). *These results are representative of the four experiments performed.*

The hematopoietic colony-forming ability of CD34+ cells was assessed by culture in methylcellulose-based semi-solid culture medium for 14 days. Three types of colonies were detected, in different numbers: BFU-E (erythroid progenitors) colonies were the less prevalent ones (17.3±1.7), followed by CFU-GEMM colonies (24.3±2.6), which are the most primitive type of colonies, and finally CFU-GM (Granulocytes, Macrophages) colonies were predominant (58.3±4.3). The fact that CD34+ cells yielded three different types of cultures suggests that they were multipotent progenitor cells. However, these results are

only preliminary since the experiment was not repeated in order to statistically distinguish the samples.

After culturing CD34⁺ cells in complete differentiation medium (EGM) for 5 days, their morphology was round, but some discrete colonies had formed **(Figure 8A)**. Still, undifferentiated CD34⁺ cells did not organize into tubular-like structures (**Figure 8B**) when cultured in Matrigel. Immunohistochemistry stainings showed that CD31 and vWF were poorly expressed (**Figure 8C-D)**, and there was no expression of VE-cadherin (**Figure 8E)**. Incorporation of Ac-LDL was also quite low **(Figure 8F)**.

After 21 days in EGM, discrete colonies had evolved into round cell clusters with spindle-shaped cells at the periphery (**Figure 9A**), and the remaining cells formed big aggregates of round cells (**Figure S-7, SD**). Also, CD34⁺-derived cells expressed EC-like features like expression of CD31 and VE-cadherin, production of vWF and incorporation of Ac-LDL **(Figure 9C-F)**, even though they did not organize into a cell monolayer or form cord-like structures in Matrigel **(Figure 9B)**.

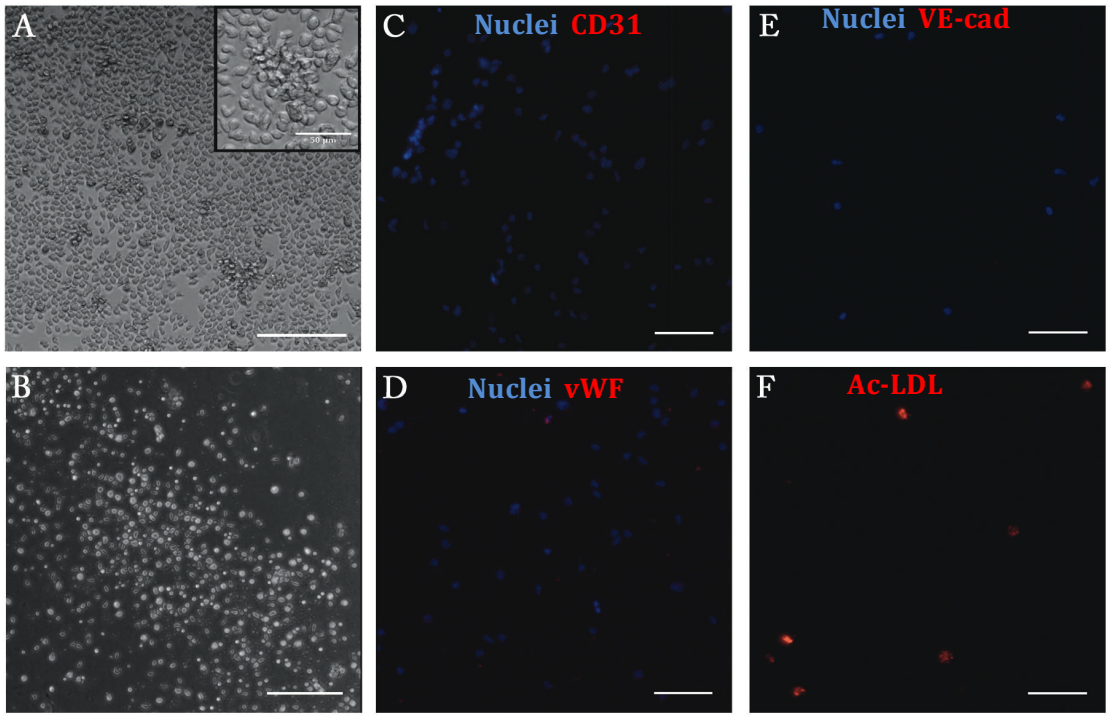

Figure 8 – CD34⁺ cells morphology and phenotypic expression after 5 days in culture. A-B: Phase contrast photomicrograph of A) CD34⁺ cells in culture, with higher magnification inset; B) cells cultured in Matrigel for 24h. *Scale bar = 150 µm, 50 µm on the inset.* **C-F:** Expression of C) CD31, D) vWF, E) VE-cadherin, and incorporation of F) Ac-LDL. *Scale bar = 50 µm*.

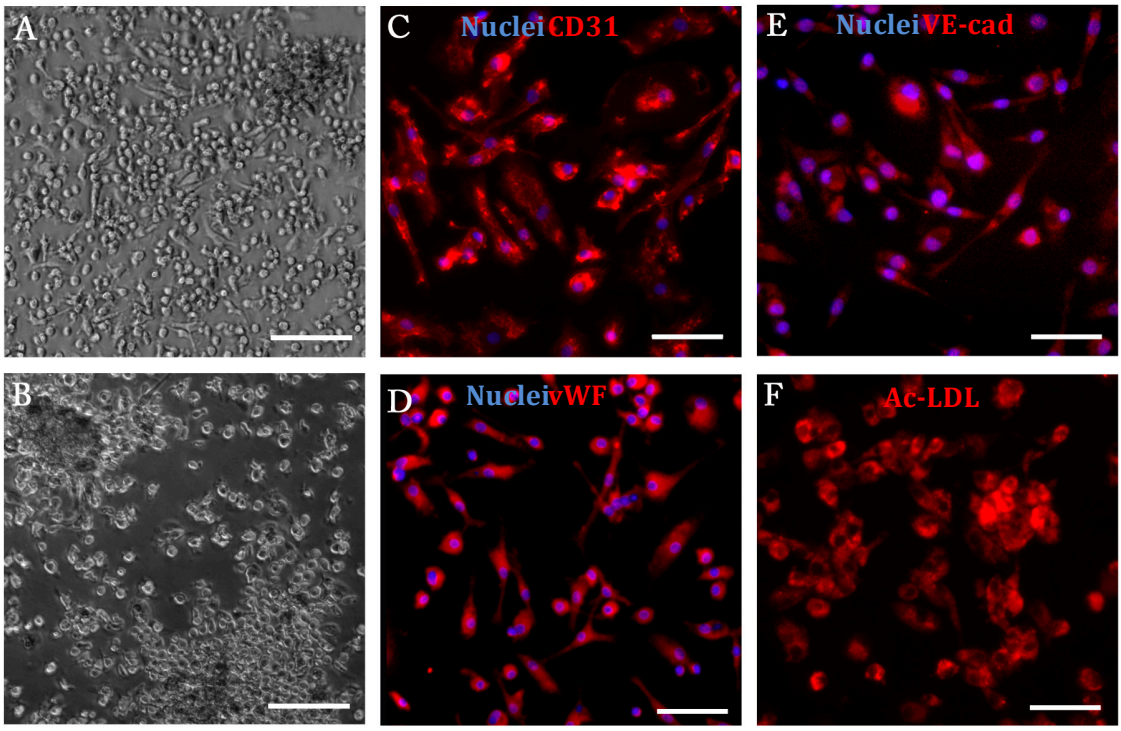

Figure 9 – CD34+-derived cells morphology and phenotypic expression after 21 days in culture. A-B: Phase contrast photomicrograph of A) CD34+-derived cells in culture; B) cells cultured in Matrigel for 24h. *Scale bar = 100 μm*. **C-F:** Expression of C) CD31, D) vWF, E) VE-cadherin, and incorporation of F) Ac-LDL. *Scale bar = 50 μm.*

DISCUSSION

Commonly, EPCs are defined as angiogenesis stimulating cells with endothelial cell features. Their angiogenic effect is a result of their ability to differentiate into mature endothelial cells and/or release paracrine stimuli, stimulating vessel formation and enhancing the formation of extracellular matrix.

CD34+ cells constitute an EPC-rich population [14]. These cells can be isolated either from peripheral or umbilical cord blood; however, they are assumed to be at a more primitive stage in the later [17], [38]. Still, they are rare [22] and their isolation, although effective (84.97±14.79% of the positively marked cell population expressed CD34), involved significant cell losses **(Figure 6)**.

First of all, the process of freezing and thawing MNCs caused cellular death, due to the presence of dimethyl sulfoxide (DMSO) in the freezing medium, which is a cryoprotectant but causes changes of osmolarity in cell suspensions, and also due to the abrupt temperature changes that might have caused lysis of the membrane of more fragile MNCs

or even other contaminating polymorphonuclear cells. Nevertheless, in these situations the percentage of $CD34^+$ cells increases, so the lost cells were not of great importance [39]. Lower cellular viability in later experiments might have resulted from a higher period of time at -80ºC, which could have irreversibly damaged the cell's membranes. Also, the isolation process (explained in **Materials and Methods**, **Section 1**) required great sensitivity from the user, especially when washing the columns (nearly all of the buffer should pass the column before more buffer was added to it, but the column could not dry) and eluting the $CD34^-$marked cells outside the magnetic field (the pressure applied to the column had to be controlled); therefore, the best results regarding the percentage of $CD34^+$ cells were obtained on later isolations, as depicted in **Figure S-3 (SD)**.

CD34 and CD31 are typically viewed as endothelial cell lineage markers; however, CD34 marks only endothelial cells and stem cell progenitors, whereas CD31+ cells can derive from the endothelial lineage or other types of MNCs (for more info, see [40]). Therefore, $CD34^+CD31^+$ marked cells are hematopoietic-lineage EPCs that express endothelial cell markers [21], [41]. On the other hand, CD38 is a cluster of differentiation that marks the majority of MNCs (lymphocytes, monocytes and macrophages), including stem cell precursors, but is not detected in endothelial cells – consequently, $CD34^+CD38^-$ cells are of an undifferentiated form – multipotent hematopoietic progenitor cells [24], [42]. According to **Table I**, the population of positively selected cells was mainly composed of hematopoietic-lineage EPCs ($CD34^+CD31^+$ cells) and the amount of hematopoietic progenitor cells ($CD34^+CD38^-$) varied a lot between donors, as the use of biological samples is always associated to high variability. Contamination with hematopoietic cells was also a risk – the percentage of $CD31^+$ cells was always higher than the percentage of $CD34^+$ cells. Luckily, most of these "contaminating" hematopoietic mononuclear cells were eluted in the first and second isolation columns (Negative 1 and 2 cell suspensions had high percentages of $CD31^+$ cells), reinforcing the utility and effectiveness of using two isolation columns.

$CD34^+$ cells reorganized into three different types of hematopoietic colonies in the colony forming unit (CFU) assay; hence, their multipotency was confirmed. Also, the fact that $CD34^+$ cells produced higher numbers of CFU-GM suggests that $CD34^+$-derived EPCs might ultimately be derived from hematopoietic cells like monocytes and macrophages, as proposed by Schmeisser et al. [43] and Rehman et al. [44].

Even though the $CD34^+$-derived cells morphology did not resemble the EC-like cobblestone appearance described by Ingram et al. [17] after 21 days, it was similar to the colony-forming EPCs morphology that is characteristic of early EPCs **(Figure 4)** [15]. Also, the expression of EC markers and the uptake of Ac-LDL were noticeably increased from

day 5 to day 21 of culture. Even though no cell-cell adherent junctions were detected, probably due to the absence of a confluent monolayer of cells, and the cells did not form tube-like structures in Matrigel, it was clear that these cells underwent endothelial commitment throughout the 21 days of incubation [20], [43]. Nonetheless, since no immunohistochemistry analysis was performed somewhere in the middle of the experiment (after 10 days, for example), it is hard to tell exactly how much time was needed for this commitment to occur.

The protocol used was based on the protocol published by Pedroso et al. [20], since their aim was also to assess the pro-angiogenic potential of CD34+ and CD34+-derived cells in 3D cultures. However, our results differed: they claimed that UCB-derived CD34+ cells differentiated into late EPCs after 21 days; yet, the data here presented suggests UCB-derived CD34+ cells yielded a population of early EPCs, which did not differentiate into mature endothelial cells but might stimulate angiogenesis by secretion of paracrine factors. Nevertheless, these results are consistent with the general definition of early EPCs [14] [15].

In vitro studies with 3D cultures

AIM

The main aim of this part of the work was to create an ideal microenvironment for EC entrapment, based on an integrative approach combining an optimized hydrogel matrix with the use of MSCs as mural cells [23]. Based on some of our group's previous results, soft RGD-grafted alginate hydrogels were used, as they have been shown to promote the self-assembly of entrapped cells (both ECs [31] and MSCs [28], and the deposition of endogenous ECM by MSCs [28]. Ideally, these matrices should assure cellular viability, support cell rearrangement and network formation, and also allow cells to migrate out from the matrices. Monocultures of HUVECs and MSCs and co-cultures of both cell types (1:1) were established and characterized at different levels. Similar assays were performed using freshly isolated $CD34^+$ cells, as a preliminary assay to evaluate the behavior of these cells in 3D culture. Due to time constraints, differentiated $CD34^+$ cells were not tested.

RESULTS:

1. HUVECS AND MSCS 3D CULTURES

1.1 METABOLIC ACTIVITY AND VIABILITY

Upon entrapment, the metabolic activity of all matrices was measured **(Figure 10)**. Whilst MSCs alone and in co-culture displayed some metabolic activity (1340 ± 305 and 2577 ± 573 RFU, respectively), HUVECs lacked it, presenting similar activity values to the blank sample. On the other hand, after being entrapped for 24 hours, the three types of cell cultures presented higher metabolic activities (3405 ± 564, 4753 ± 194 and 9662 ± 291 RFU, respectively). After 72 hours, HUVECs/MSCs cultures maintained their activity (10200 ± 400 RFU), whilst the activity of HUVECs and MSCs monocultures decreased slightly (2461 ± 1395 and 3490 ± 382 RFU, respectively).

After 24 hours in culture, all conditions had a few dead cells, as evaluated by the Live/Dead assay **(Figure 11)**, but HUVECs-laden matrices were the ones with the lowest viability. Importantly, the overall survival of HUVEC appeared to be increased by the presence of MSCs. Also, while in monocultures live HUVECs and MSCs exhibited a predominantly round shape and were individually distributed along the matrix, live cells in co-culture seemed to spread to some extent, and established contacts with other cells.

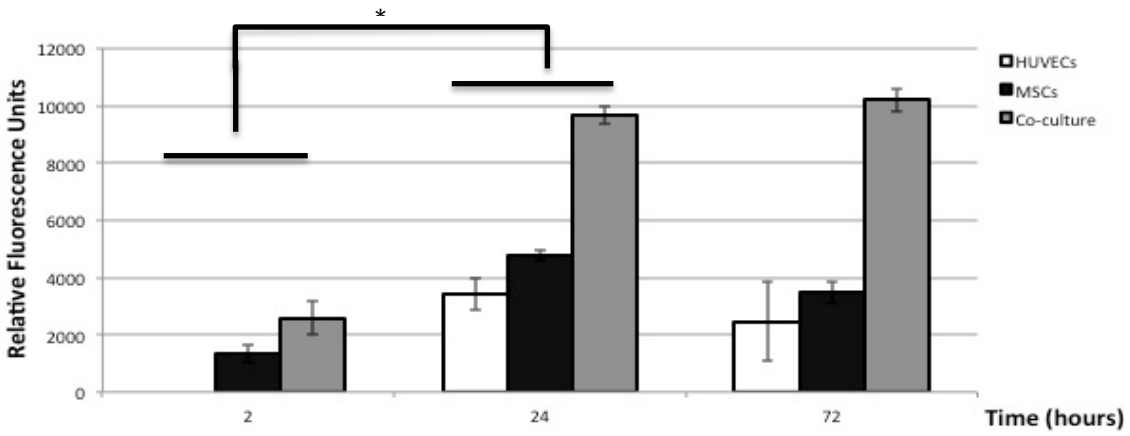

Figure 10 – Metabolic activity of HUVECs/MSCs 3D cultures throughout a 3-day culturing period. Metabolic activity was severely increased from day 0 (2 hours) to day 1 (24 hours) and maintained from thereon. *All values are relative to blank sample (EGM). * means p is <0.05.*

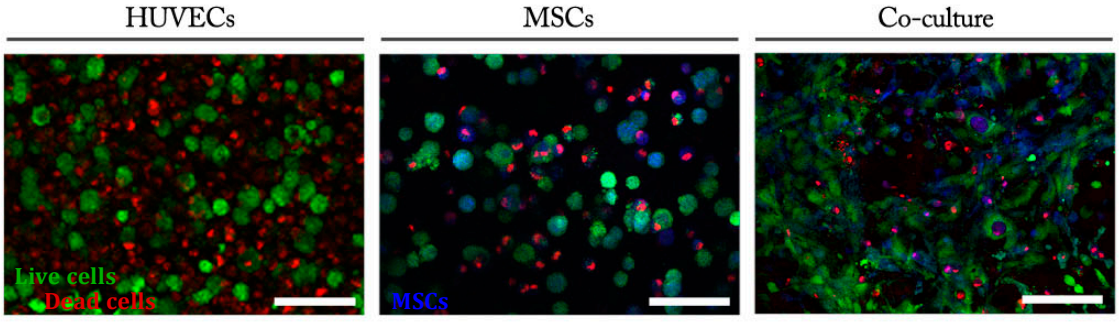

Figure 11 – Live/Dead Assay 24 hours after cell embedment. The percentage of dead cells was especially high in the monocultures. In co-culture, live cells were stretched. *Scale bar = 100 µm. One sample per condition was analyzed, under confocal fluorescence microscope.*

1.2. CELL REARRANGEMENT AND MATRIX FORMATION IN HUVECs/MSCs 3D CULTURES

All of the hydrogel matrices suffered some cell-driven reduction in their diameter, but this was specially observed co-cultured constructs, which were reduced to almost half (54%) of their initial diameter after 72 hours in culture **(Figure 12).** HUVECs and MSCs in monoculture caused minimal diminishment of the matrices diameter (86% and 83% of the initial diameter, respectively), which kept a soft and fragile consistency at all times.

In order to better analyze the relative spatial organization of both cell types in co-culture, MSCs were pre-labeled with CellTraker Blue before entrapment, while HUVECs were labeled by incorporation of DiI-Ac-LDL (red) at the end of the culture. Moreover, cytoskeleton re-organization was analyzed by f-actin staining with a fluorescent dye (green). Important differences were observed between monocultures (data not shown) and co-cultures. As depicted **in Figure 13**, HUVECs and MSCs in co-culture reorganized so that instead of remaining round and isolated (2 hours), they spread (24 hours) and formed multi-cellular networks of increasing complexity (24 and 72 hours) **(Figure 12)**.

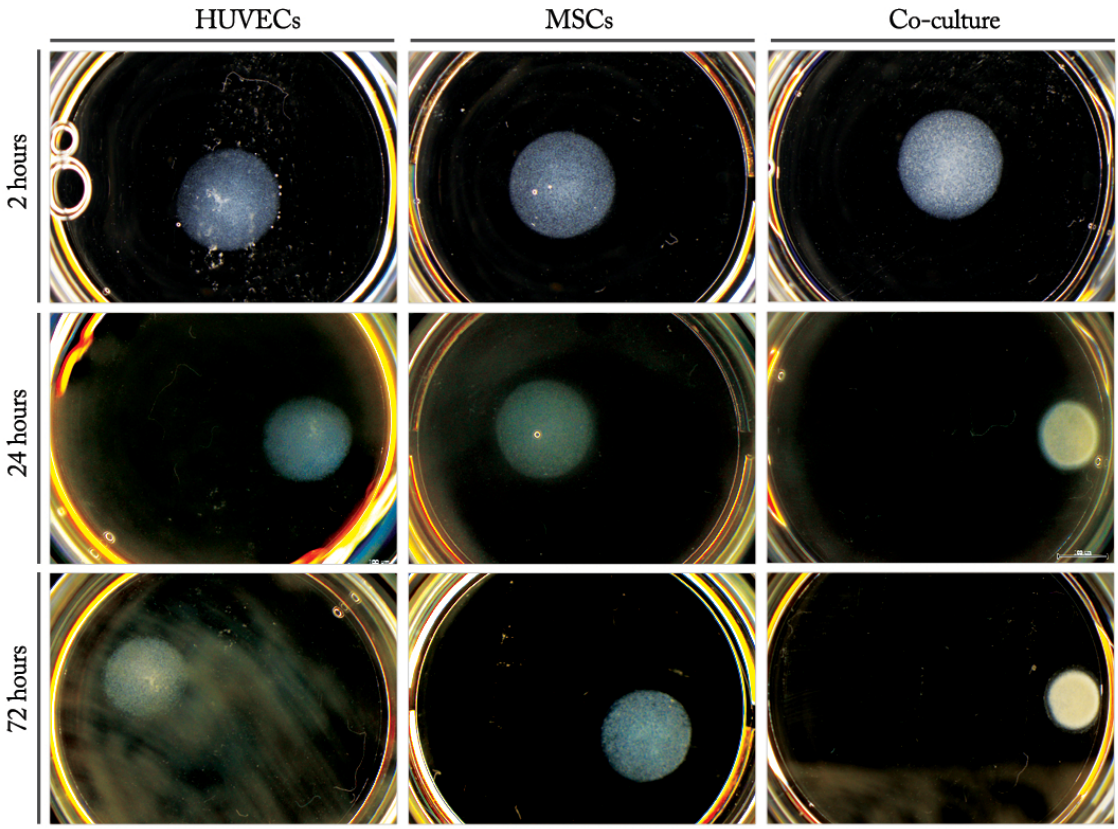

Figure 12 – General appearance of alginate hydrogel disks 2, 24 and 72 hours after cell embedment. All of the disks diameters were diminished; however, co-cultured disks displayed drastic differences and formed dense aggregates. *Photos were taken using a stereoscopic microscope; each cell culture is represented by one disk, photographed at 3 different time-points.*

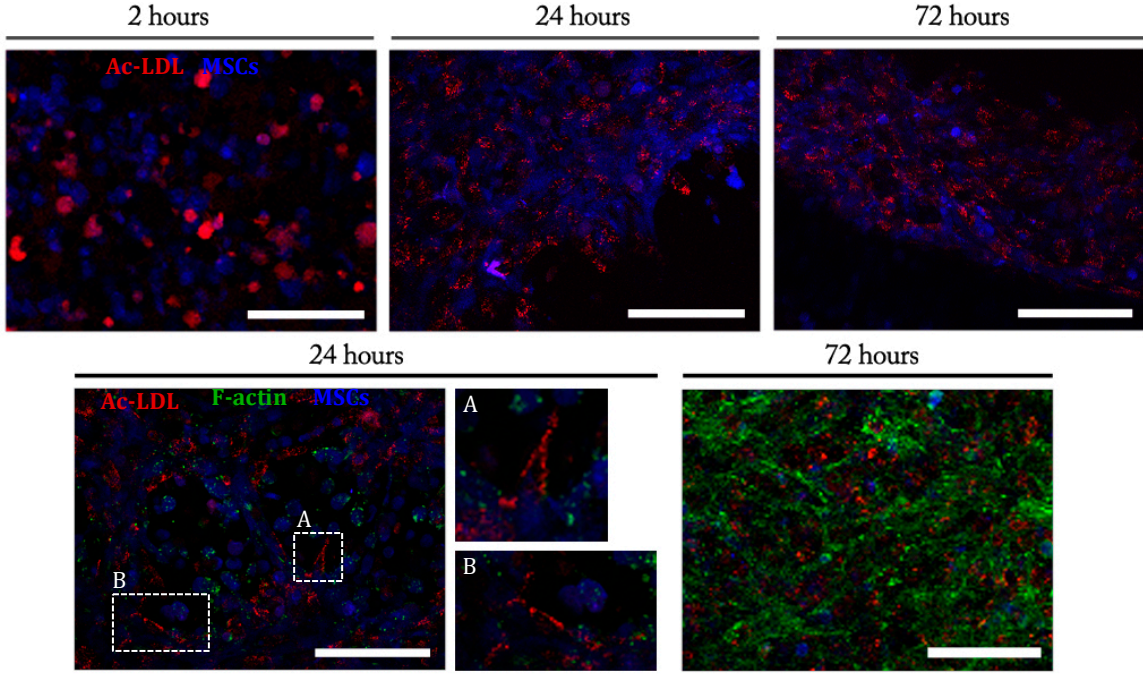

Figure 13 – Morphology and spatial organization of HUVECs and MSCs in 3D co-culture. Both types of cells rearranged inside the matrix and started expressing F-actin 24 hours after incubation. F-actin microfilaments were detected after 72 hours. Some ECs were able to align into tubular-like structures. *Different samples were used for each time point. Whole-mounted samples were visualized under confocal fluorescence microscope. Scale bar=150 µm.*

Expression of F-actin was detected after 24 hours (apparently mostly by MSCs, taking into account the co-localization of blue/green staining), and after 72 hours F-actin microfilaments were clearly visible around MSCs and HUVECs. More importantly, the co-culture microenvironment induced ECs to assemble into cord-like structures (aligned ECs depicted in A and B insets), and permitted a close-proximity of both cell types.

The expression of fibronectin (FN) was also analyzed, as this ECM protein plays a key role in the promotion of cell-matrix interactions and in the stabilization of multicellular structures [45]. When seeded alone, HUVECs and MSCs did not reorganize into multi cellular structures, but some FN expression was detected mainly intracellularly **(Figure 14)**. The expression of both FN and F-actin increased from 24 to 72 hours. Conversely, after 24 hours in co-culture, cells were predominantly spread, as supported by the presence of organized F-actin microfilaments, and were able to assemble an extracellular FN-matrix. Ultimately, after 72 hours **(Figure 15)** cells in co-culture formed a multicellular network, embedded in a FN mesh.

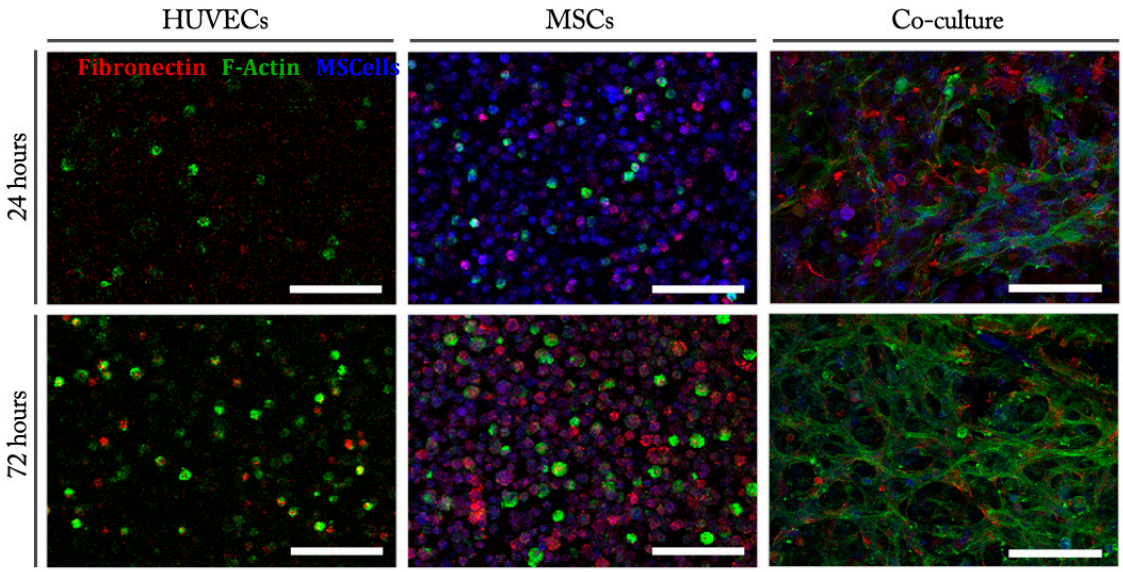

Figure 14 – Extracellular matrix and multicellular networks in HUVECs/MSCs 3D culture. No networks were detected in monocultures; however, MSCs produced higher amounts of FN. Co-cultured cells formed multicellular networks and a fibronectin matrix. *Different samples were stained at each time point; samples were visualized under confocal fluorescence microscope. Scale bar=150 μm.*

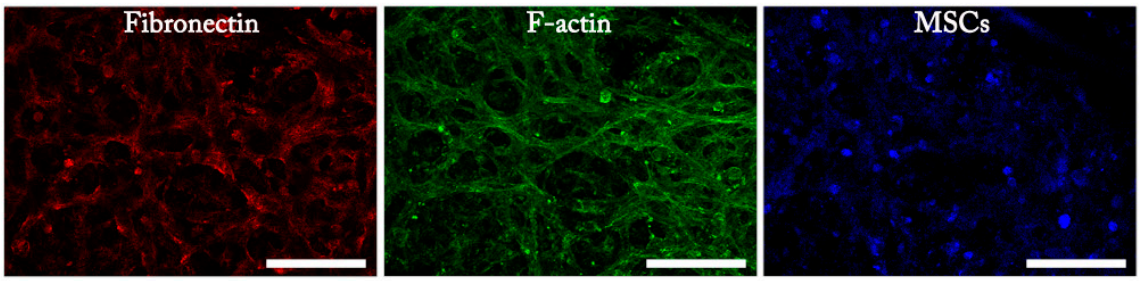

Figure 15 –Decomposed confocal fluorescent microscopy image of 3D HUVECs/MSCs culture after 72 hours. *Scale bar=150 μm.*

1.3. OUTWARD CELL MIGRATION

To evaluate the ability of entrapped cells to migrate out from the matrices, cell-laden hydrogel discs were prepared and immediately embedded into a tissue mimic (Matrigel, **Figure S-2**, in **SD**). As depicted in **(Figure 16, days 1 and 2),** some HUVECs protruding from monoculture matrices were visible after 1 day of culture (orange arrows), which formed tubular-like structures that invaded the Matrigel, but these were no longer present after 2 days of culture. On MSC monocultures only a few sprouting MSCs were found even after 2 days of culture. In co-cultured discs, numerous migrating cells with spread

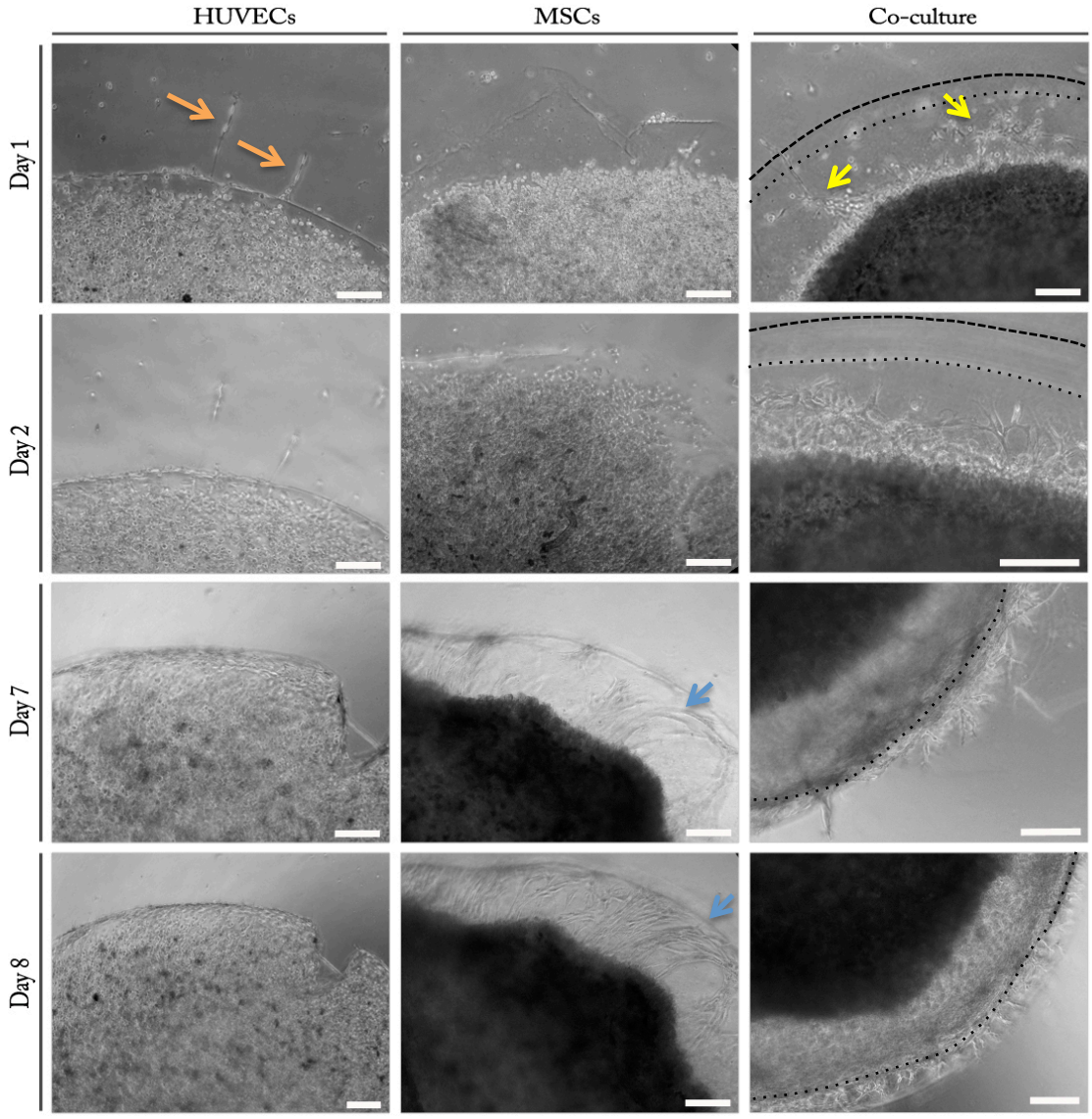

Figure 16 – Representative phase-contrast micrographs of cell-laden disks embedded in Matrigel. Cell migration and stretching was significantly increased when HUVECs and MSCs were co-cultured, before and after a period in EGM. *One representative sample is shown per type of culture. Samples were visualized under inverted microscope. Scale bar=200 µm.*

morphology were detected at the periphery of the alginate disc (yellow arrows), which increased from day 1 to day 2. Unfortunately, although both MSCs and HUVECs were successfully labeled with CellTracker (Blue and Green, respectively) before entrapment **(as seen in Figure S-7, in SD)**, it was not possible to differentiate them amongst the migrating cells population, as the sprouting structures could not be visualized by fluorescence microscopy. Also, the previously described matrix contraction **(Section 1.2)** generated a gap between the discs periphery and Matrigel (dotted and dashed lines, respectively), especially in co-cultured constructs causing, inclusively, some discs to detach from the Matrigel layer. Moreover, as time in cultured progressed, the Matrigel started to degrade. Altogether, these technical difficulties did not allow a more thorough interpretation of the obtained results. The same discs were then re-cultured in EGM for an additional period of 4 days, to allow full disc contraction, before placing them again in Matrigel at Day 6. Along the 4-days incubation period, the metabolic activity of the entrapped cells increased in all the culture conditions **(Figure 17)**. Effectively, some additional matrix contraction was observed after the 4-days period, not only in co-cultures but also in MSC monocultures. After 24 hours (Day 7) of re-implantation in Matrigel **(Figure 16**), MSC at the periphery of alginate discs stretched out about 400 μm onto the interface of the disc with Matrigel **(Figure 16**, Day 7, blue arrows). However, these structures did not seem to invade the Matrigel layer and did not further developed after 1 more day in culture (Day 8). In HUVECs monocultures, no cell migration was detected. Contrarily, in co-cultures at Day 7, numerous migrating cells were present at the disc periphery, and invaded the Matrigel layer. After 48 hours in Matrigel (Day 8), the entire construct was surrounded by sprouting cells.

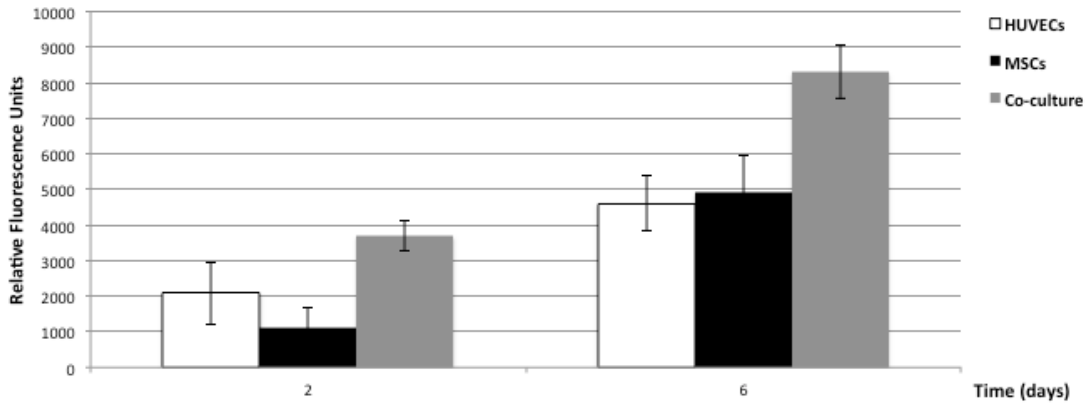

Figure 17 – Metabolic activity of cell-seeded alginate disks before and after culture in EGM. The metabolic activity of the three types of culture was increased when they were left in culture for 4 days. *The experiment was performed once, in triplicate for each condition.*

2. CD34$^+$ CELLS AND MSCS 3D CULTURES

2.1. METABOLIC ACTIVITY AND VIABILITY

Moving on to the characterization of CD34+ cells in a 3D environment, CD34+ cells, MSCs, and their co-culture (1:1 ratio) were embedded in alginate hydrogel discs. According to their metabolic activity readings **(Figure 18)**, MSCs activity decreased with time (8832 ± 148, 8740 ± 1621 and 3479 RFU for 2, 24 and 72 hours respectively) and CD34+ cells did not exhibit metabolic activity at any time points (at 2 hours, the activity was 250 ± 52 RFU, which is nearly 0). The activity in co-cultures was smaller than in MSCs after 2 hours (5184 ± 363 RFU), but it increased after 24 hours (8478 ± 205 RFU) and decreased after 48 hours (6605 ± 278 RFU).

When CD34+ cells and MSCs were cultured alone, they presented abnormally high numbers of dead cells after 24 hours **(Figure 19)**. Even though initially CD34+/MSCs constructs had the highest viability, it decreased significantly on the following 48 hours; however, based on their smaller size, it seems most of the dead cells in co-culture are CD34+ cells.

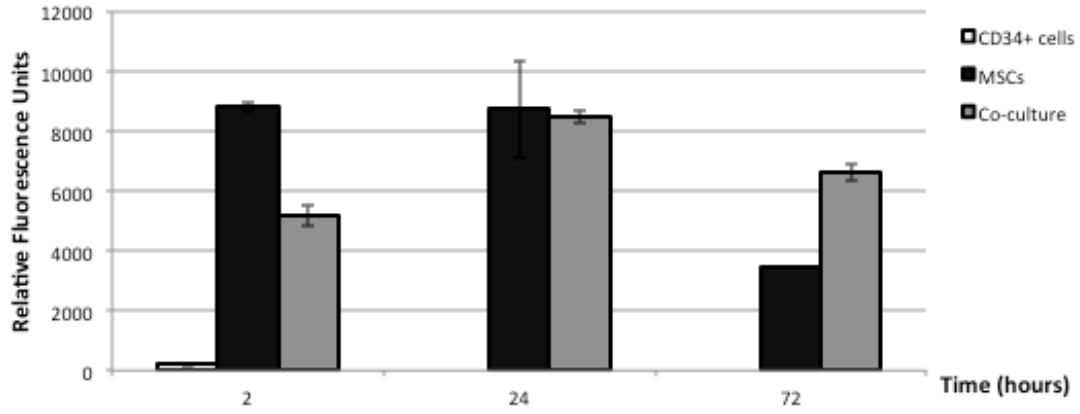

Figure 18 – Metabolic activity of CD34+ cells/MSCs 3D cultures throughout a 3-day culturing period. The activity of co-cultured cells increased from day 0 (2 hours) to day 1 (24 hours) and decreased afterwards. MSCs activity decreased with time, and CD34+ cells activity was null or close to it at all time-points. *The experiment was performed once, and the bars without standard deviation represent values obtained from 1 or 2 samples only.*

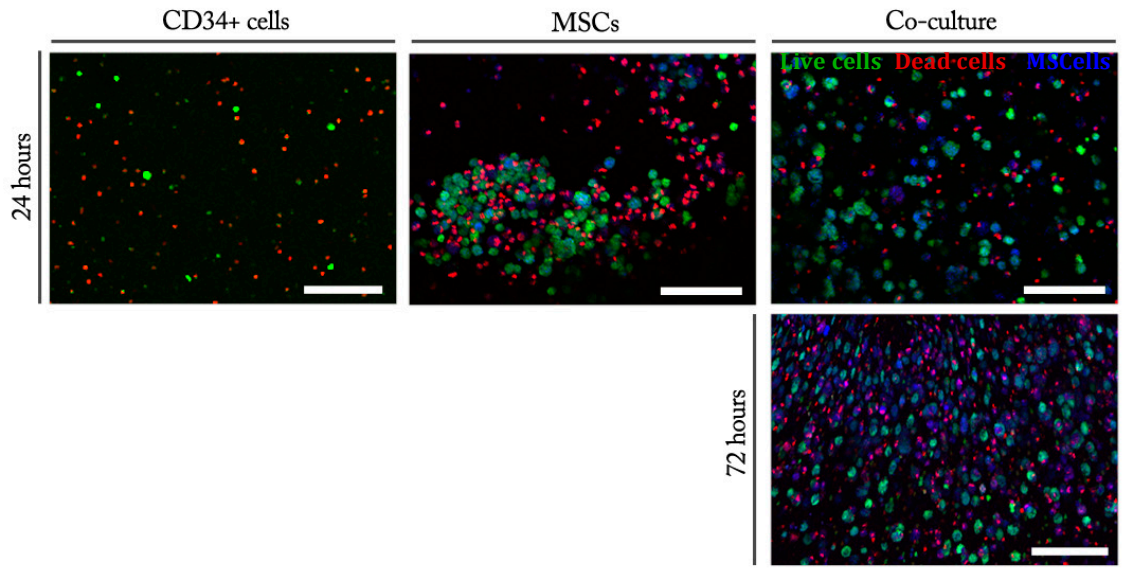

Figure 19 – Live/Dead Assay – 24 and 72 hours after cell embedment. After 24 hours of incubation, a great fraction of monocultured cells were dead. The same remains true for co-cultures after 3 days in culture, where most of the dead cells seem to be $CD34^+$ (smaller size). *Scale = 150 μm. Different samples were sacrificed at different time-points, and visualized under confocal fluorescence microscope.*

2.2. CELL REARRANGEMENT AND MATRIX FORMATION IN $CD34^+$ CELLS/MSCs 3D CULTURES

Based on the low cell viability in monoculture constructs, the following assays were only performed on co-cultured discs. When cultures were incubated with DiI-Ac-LDL after 24 hours, no evident differences were detected between marked MSCs and $CD34^+$ cells; there seemed to be a residual uptake of Ac-LDL from all cells. After 72 hours, $CD34^+$ cells were distinguishable from MSCs through a much stronger staining and their smaller size **(Figure 20)**. Still, no rearrangement or co-localization of the two types of cells was detected at any time point. Expression of both F-actin and FN was detected after 24 and 72 hours, and some cells spread and formed networks while other remained essentially round. Although it is not easy to distinguish between the two cell types, looking at the cell size and the pattern of F-actin staining, it seems that the spread cells are mainly MSC. FN was detected at 24 hours, but FN fibrils were only detected at 72 hours and in very low amounts (white arrows)

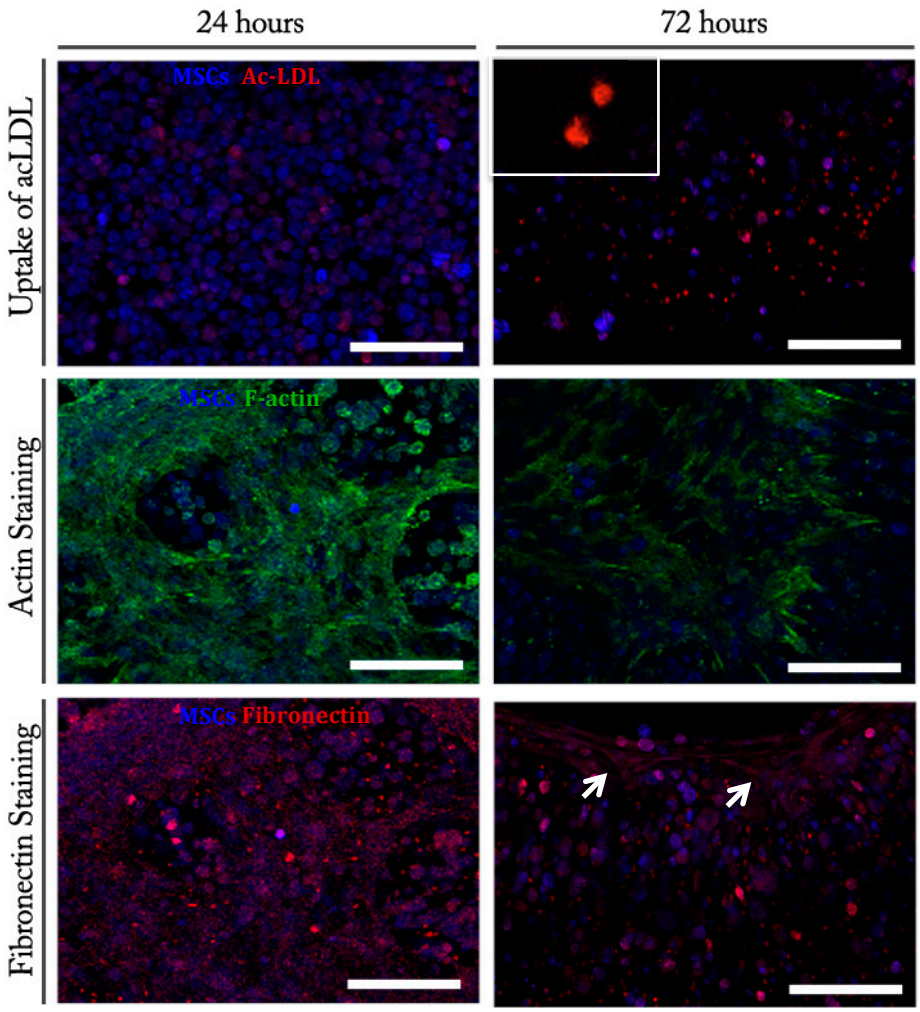

Figure 20 – Cell functionality, morphology and extracellular matrix production in CD34⁺ cells/MSCs 3D culture. CD34⁺ cells clearly incorporate Ac-LDL after 72 hours in culture (inset). Extracellular actin fibers are detected after 24 hours, whilst fibronectin secretion is much lower. White arrows: FN fibrils. *Different samples were used at each time point and for each assay (Ac-LDL uptake and fibronectin/actin staining). The constructs were visualized under confocal fluorescence microscope. Scale bar=150 µm.*

DISCUSSION:

1. HUVECs/MSCs 3D CONSTRUCTS:

In this study, a previously optimized soft RGD-grafted alginate hydrogel was studied as a 3D matrix for the culture of ECs. The final goal is the development of a vehicle for therapeutic endothelial cell delivery and angiogenesis stimulation. In the past, HUVECs 3D-monocultures were already successfully established using this hydrogel formulation that, in contrast to non-modified alginate hydrogels (without RGD), was shown to promote the internal formation of multicellular ECs networks and the outward migration of ECs into Matrigel, with tube-like structures formation [31]. On the other hand, the same

formulation was previously shown to promote the formation of MSCs networks, with endogenous ECM (FN-rich) deposition [28]. Therefore, in an attempt to create an ideal microenvironment for EC entrapment [46], here we decided to test an integrative approach combining this optimized hydrogel matrix with the use of co-entrapped MSCs as mural cells.

The selected cell density was 5 x 10^6 cells/mL of each cell type, yielding a concentration of about 10 x 10^6 cells/mL on the co-cultured discs. After the first 2 hours post-entrapment, all of the cultures seemed to be at a steady, adaptive state (especially HUVECs). The metabolic activity increased after 24 hours, and then remained nearly constant until the end of the culture. However, the metabolic activity in co-cultures plateaued between day 1 and day 3, whilst monocultures activity slightly decreased, so there seemed to be a beneficial effect of HUVECs and MSCs over each other, even though the relative contribution of each cell type could no be discriminated. In what concerns cell viability, HUVECs monocultures presented a significant percentage of dead cells, contrary to that observed by Bidarra et al., who previously reported that the viability of HUVECs within these matrices gradually decreases with time, but remaining high (80%) after 3 days of culture [11]. These discrepancies may be a consequence of the different cell densities that were used (5 x 10^6 cells/mL vs. 20 x 10^6 cells/mL). Also, previous studies with MSCs entrapped within similar 3D matrices reported more significant discs compaction after 24 hours (around 48%) [28] that, again, might be due to the different cell densities used here and in that study (5 x 10^6 cells/mL vs. 8 x 10^6 cells/mL).

Cell rearrangement into networks and deposition of FN-rich ECM in co-cultured constructs confirmed that cells were able to adhere to the polymeric matrix, spread and establish cell-cell contacts. Even though HUVECs were not labeled in these assays, the F-actin and FN network layouts suggest they were also involved in these structures. The fact that cellular networks were not detected in HUVECs or MSCs monocultures, even though they were at the same individual cell density in the co-culture and were able to form cellular networks in other experiments [28], [31], highlights the importance of cell density optimization. Also, the culture medium we used could be optimized, not only by adjusting the growth factors used, but also by testing other media, like MSCGM, which was used by Maia et al. on the assays with MSCs [28]. Nevertheless, in co-cultures cells were able to connect and assemble a FN mesh, which appears to be a quite interesting feature as it has been established that FN fibrillogenesis regulates 3D neovessel formation, namely by serving as a structural scaffolding that displays adhesive ligands on an mechanically ideal substratum [47]. Also, the close-proximity of the two cells types in co-culture is likely to

foster their interaction, which is also essential if MSCs are aimed to act as pericyte-like supporting cells [27], [48], [49].

Overall, as suggested by Maia et al. [28], when cells were entrapped within very soft alginate hydrogels they seemed to be able to rapidly modify their local mechanical and biochemical environment, become embedded and ultimately reside within a self-synthesized ECM.

Culturing the disks in EGM before repeating the migration assay led more cells from the co-culture to migrate once they were in Matrigel. Even though the detected migrating sprouts were similar to MSCs sprouts, the fact that cellular migration was only relevant on HUVECs/MSCs constructs emphasizes the importance of co-cultures. Also, HUVECs loss of ability to form networks (hence, spread) after a few days in culture had been previously reported by Moon et al., in PEG hydrogels [50]. The fact that co-culture loaded constructs had higher sprout formation after a period in culture suggests that there might be advantages in pre-culturing the cell-laden constructs before implanting them *in vivo*, as the presence of a mature network within the construct can potentially yield better results [7].

2. $CD34^+$ CELLS/MSCS 3D CULTURE

As previously described, similar assays were performed using freshly isolated $CD34^+$ cells, as a preliminary assay to evaluate the behavior of these cells in 3D culture. Cells were assayed not only in monoculture, but also co-cultured with MSC, as these cells not only play an important role in angiogenesis, but also improve the expansion of hematopoietic stem cells and $CD34^+$ progenitor cells [51]. When embedded in soft RGD-alginate matrices, $CD34^+$ cells presented a nearly null metabolic activity at all times. This behavior had already been reported by Chen et al. [48], who cultured EPCs on a different polymer and concluded that those cells did not proliferate and also lost viability with time. However, from day 1 to day 3, the metabolic activity of co-cultures decreased much less than that of MSCs monocultures, suggesting that the co-culture has a beneficial effect on one (or the two) cell types. Otherwise the behavior of the co-cultured constructs would be similar to the MSCs. For example, $CD34^+$ cells proliferation might eventually be increased when these were co-cultured with MSCs, as described by Walenda et al.[24]. F-actin networks seemed smaller but more organized after 72 hours than after 24 hours. Chen et al. had previously reported that the presence of ECFCs (late EPCs) diminished the extent of MSCs spreading and their proliferation [48]. Another interesting feature was that, even

though the constructs viability was low, co-cultured $CD34^+$ cells started to incorporate Ac-LDL after 72 hours in culture, what suggests that they did not completely lose their functionality, and eventually started to acquire an endothelial-like phenotype [4]. When compared to HUVECs, $CD34^+$ cells seemed to be more "dependent", in the way that most of the times they need other type of cells to support their function and/or stimulate their differentiation [20], [23]. These assumptions are obviously quite speculative and it would be important to repeat these experiments in future studies, using more biological replicates, to draw more valid conclusions.

In vivo studies with 3D cultures

AIM:

The aim of this part of the work was to make a preliminary evaluation of the *in vivo* angiogenic potential of cell-laden soft RGD-alginate. Specific targets were to: (1) compare the effect of 3D co-cultures vs. monocultures; and (2) evaluate whether a pre-culture time improves the system's performance. The chorioallantic membrane (CAM) assay was chosen as the *in vivo* model due to its previously described advantages, and because it has been previously used to assess the efficiency of other cell-laden hydrogels in inducing capillary formation [37]. This study will function as a bridge between 3D *in vitro* assays and *in vivo* mammalian models [36]. Here, differences between HUVECs/MSCs 3D mono- and co-cultures (1:1) in soft RGD-alginate hydrogel matrices were assessed, with and without a 5-day pre-culturing period.

RESULTS:

Cell-laden 3D matrices prepared on the same day as the implantation and 5 days before (kept in EGM) were tested. Pre-cultured HUVECs monocultures were not tested, due to technical problems. As previously described, matrices with co-cultures and MSC monocultures suffered contraction throughout those 5 days in culture, which resulted in denser disks upon implantation. After 3 days, the CAM was fixed with PFA and the part of the membrane containing the scaffold was photographed, with and without the O-ring. One of the embryos (with a co-cultured construct) died. From their gross evaluation, all samples seemed to be incorporated into the CAM quite well and capillary vessels grew towards and underneath all disks **(Figure 21)**. New capillary vessels that were stimulated by the presence of the constructs were identified as zigzag vessels, sprouting from the parent vessel and directed towards the disk, changing th eir ordinary growth pathway **(Figure 22)**. This step is the first and determinant step in angiogenesis stimulation, so these are the vessels that represent the construct's influence on the CAM. Surprisingly, no differences were detected between the different culture types, but the angiogenesis stimulation seemed to be improved in pre-cultured disks. Unfortunately, the experiment was only repeated once and the number of samples was not enough to yield a definite conclusion (only MSCs with and without previous culturing time had statistically different numbers of vessels formed).

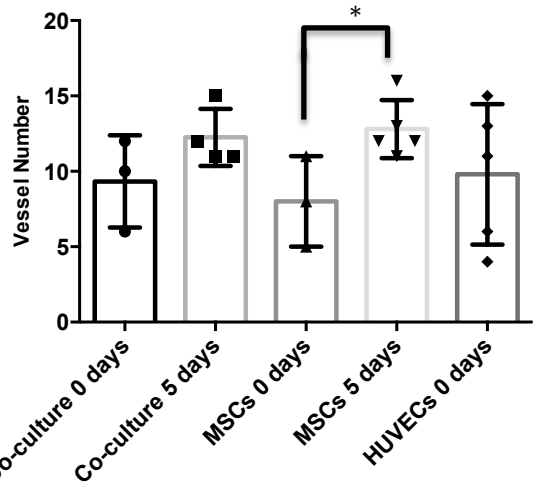

Figure 21 – Effect of different cell cultures and pre-incubation of alginate hydrogel disks on blood vessel density in CAM assay without VEGF. Even though the number of formed vessels seemed to be increased on constructs previously cultured, a significant difference was noticed in MSCs only ($p < 0.03$) due to the small number of samples (n=4 for MSCs 0 days and n=5 on all other conditions). No difference was detected amongst different types of cells. *The data shown are mean ± SD. * means statistically different ($p<0.05$).*

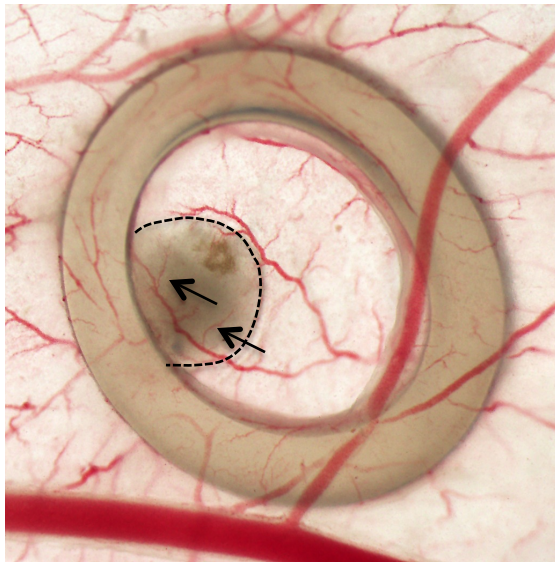

Figure 22 – Photograph of representative CAM of 13 day-old chick embryo (Day 3 after implantation). The O-ring (5 mm diameter) kept the disks in place and facilitated the visualization of vasculature around it. *Samples were photographed under a stereoscopic microscope with 2x amplification. Black arrows indicate new capillary vessels in pre-cultured MSCs-laden disks, dotted line surrounds the disc.*

5.3. DISCUSSION:

A CAM assay with alginate disks containing HUVECs, MSCs and their 3D co-cultures was performed in order to assess their efficiency in inducing capillary formation in vivo. Pre-cultured (5 days) and fresh constructs were implanted to detect if there is an advantage in implanting constructs with a mature network of cells and extracellular proteins, as previously described by others [7]. While all of the samples stimulated capillary formation, even in the absence of exogenous VEGF supplementation, no differences were found between the different types of cultures. In the future, it would be important to increase the implantation time, and also run a control of acellular soft RGD-grafted alginate hydrogels to see if the matrix has any bioactive effect by itself. Actually, there seemed to be an increased stimulation in all samples that were pre-cultured, suggesting it might be advantageous to implant more mature cellular structures.

However, these results were only preliminary and the experiment would have to be repeated in order to validate these conclusions and give them a statistical meaning.

Main conclusions and future prospects

Towards the development of a pro-angiogenic cells-delivery vehicle, the main aim of this work was to create an ideal microenvironment for EC entrapment using an integrative approach, combining an optimized hydrogel matrix with the use of co-entrapped MSCs as mural cells.

Regarding UCB-derived $CD34^+$ cells, these cells seemed to differentiate into early EPCs, which present a different phenotype from mature endothelial cells. However, according to what is already known about EPCs, these cells might stimulate angiogenesis by secretion of paracrine factors. In the future it would be interesting to test $CD34^+$ cells and $CD34^+$-derived EPCs conditioned media in terms of their ability to stimulate tubule-formation by HUVECs in a Matrigel assay. It would also be enlightening to evaluate the markers expression by flow cytometry not only using more markers, like AC133 that is not expressed in mature ECs [52], but also in $CD34^+$-derived EPCs.

This study suggests that the combination of soft RGD-alginate matrices with co-entrapped MSC might in fact be a suitable strategy to create an adequate 3D microenvironment for ECs. If seeded with the right cell types at optimized densities, these hydrogels can not only support cells metabolic activity and viability, but also promote cell-cell interactions and formation of multicellular networks stabilized by an organized FN-rich extracellular matrix. These constructs also allowed the outward migration of embedded cells and cell sprouting through a tissue mimic, which is a key feature of a cell delivery system. The relevance of co-culturing $CD34^+$ cells with MSCs was also confirmed as both seemed to exert some influence over each other. However, before more studies are performed, it would be important to optimize the culturing conditions for this particular cell type, namely in terms of matrix formulation.

In the future, it will be crucial to repeat these 3D assays and further optimize the culturing conditions, specifically regarding cell density. For example, it would be interesting to incorporate the same number of cells in all samples, regardless of the type of cell culture. Leaving the samples for a longer period of time in culture could also yield more answers regarding their progressive reorganization. Also, MSCs could be labeled with pericyte markers like smooth muscle myosin, in order to evaluate if they effectively acquire a pericyte-like phenotype and start lining the ECs tubular structures. Conclusively, it might be interesting to evaluate the potentially synergistic effect of co-delivering specific growth factors [34] or performing tri-cultures of mature ECs with EPCs and supporting cells, like MSCs.

Last but not least, the *in vivo* assay suggested that soft RGD-alginate hydrogels with embedded cells actually stimulate the formation of new blood vessels. Also, it implied that there might be a beneficial effect in pre-culturing the cell-laden matrices before implantation. However, these results were only preliminary and this assay should be repeated with more samples after the culturing conditions are optimized.

References

[1] E. C. Novosel, C. Kleinhans, and P. J. Kluger, "Vascularization is the key challenge in tissue engineering," *Advanced drug delivery reviews*, vol. 63, no. 4, pp. 300–311, Apr. 2011.

[2] M. E. Lukashev and Z. Werb, "ECM signalling: orchestrating cell behaviour and misbehaviour.," *Trends Cell Biol.*, vol. 8, no. 11, pp. 437–441, Nov. 1998.

[3] A. Page-McCaw, A. J. Ewald, and Z. Werb, "Matrix metalloproteinases and the regulation of tissue remodelling.," *Nat Rev Mol Cell Biol*, vol. 8, no. 3, pp. 221–233, Mar. 2007.

[4] T. Asahara and A. Kawamoto, "Endothelial progenitor cells for postnatal vasculogenesis," *American journal of physiology. Cell physiology*, vol. 287, no. 3, pp. C572–9, Sep. 2004.

[5] C. J. Drake, J. E. Hungerford, and C. D. Little, "Morphogenesis of the first blood vessels.," *Annals of the New York Academy of Sciences*, vol. 857, pp. 155–179, Oct. 1998.

[6] N. C. Rivron, J. J. Liu, J. Rouwkema, J. de Boer, and C. A. van Blitterswijk, "Engineering vascularised tissues in vitro," *European cells & materials*, vol. 15, pp. 27–40, 2008.

[7] J. Koffler, K. Kaufman-Francis, Y. Shandalov, D. Egozi, D. A. Pavlov, A. Landesberg, and S. Levenberg, "Improved vascular organization enhances functional integration of engineered skeletal muscle grafts," *Proceedings of the National Academy of Sciences of the United States of America*, vol. 108, no. 36, pp. 14789–14794, Sep. 2011.

[8] S. Soker, M. Machado, and A. Atala, "Systems for therapeutic angiogenesis in tissue engineering," *World journal of urology*, vol. 18, no. 1, pp. 10–18, Feb. 2000.

[9] M. P. Lutolf and J. A. Hubbell, "Synthetic biomaterials as instructive extracellular microenvironments for morphogenesis in tissue engineering," *Nature biotechnology*, vol. 23, no. 1, pp. 47–55, Jan. 2005.

[10] I. Sukmana, "Microvascular guidance: a challenge to support the development of vascularised tissue engineering construct," *TheScientificWorldJournal*, vol. 2012, p. 201352, 2012.

[11] S. J. Bidarra, C. C. Barrias, M. A. Barbosa, R. Soares, and P. L. Granja, "Immobilization of human mesenchymal stem cells within RGD-grafted alginate microspheres and assessment of their angiogenic potential.," *Biomacromolecules*, vol. 11, no. 8, pp. 1956–1964, Aug. 2010.

[12] C. Kalka, H. Masuda, T. Takahashi, W. M. Kalka-Moll, M. Silver, M. Kearney, T. Li, J. M. Isner, and T. Asahara, "Transplantation of ex vivo expanded endothelial progenitor cells for therapeutic neovascularization," *Proceedings of the National Academy of Sciences of the United States of America*, vol. 97, no. 7, pp. 3422–3427, Mar. 2000.

[13] T. Asahara, T. Murohara, A. Sullivan, M. Silver, R. van der Zee, T. Li, B. Witzenbichler, G. Schatteman, and J. M. Isner, "Isolation of putative progenitor endothelial cells for angiogenesis.," *Science*, vol. 275, no. 5302, pp. 964–967, Feb. 1997.

[14] T. Asahara, A. Kawamoto, and H. Masuda, "Concise review: Circulating endothelial progenitor cells for vascular medicine," *Stem cells*, vol. 29, no. 11, pp. 1650–1655, Nov. 2011.

[15] D. N. Prater, J. Case, D. A. Ingram, and M. C. Yoder, "Working hypothesis to redefine endothelial progenitor cells.," *Leukemia*, vol. 21, no. 6, pp. 1141–1149, Jun. 2007.

[16] D. P. Sieveking, A. Buckle, D. S. Celermajer, and M. K. Ng, "Strikingly different angiogenic properties of endothelial progenitor cell subpopulations: insights from a novel human angiogenesis assay," *Journal of the American College of Cardiology*, vol. 51, no. 6, pp. 660–668, Feb. 2008.

[17] D. A. Ingram, L. E. Mead, H. Tanaka, V. Meade, A. Fenoglio, K. Mortell, K. Pollok, M. J. Ferkowicz, D. Gilley, and M. C. Yoder, "Identification of a novel hierarchy of endothelial progenitor cells using human peripheral and umbilical cord blood," *Blood*, vol. 104, no. 9, pp. 2752–2760, Nov. 2004.

[18] M. C. Yoder, L. E. Mead, D. Prater, T. R. Krier, K. N. Mroueh, F. Li, R. Krasich, C. J. Temm, J. T. Prchal, and D. A. Ingram, "Redefining endothelial progenitor cells via clonal analysis and hematopoietic stem/progenitor cell principals," *Blood*, vol. 109, no. 5, pp. 1801–1809, Mar. 2007.

[19] J. Yang, M. Ii, N. Kamei, C. Alev, S. M. Kwon, A. Kawamoto, H. Akimaru, H. Masuda, Y. Sawa, and T. Asahara, "CD34+ cells represent highly functional endothelial progenitor cells in murine bone marrow," *PloS one*, vol. 6, no. 5, p. e20219, 2011.

[20] D. C. Pedroso, A. Tellechea, L. Moura, I. Fidalgo-Carvalho, J. Duarte, E. Carvalho, and L. Ferreira, "Improved survival, vascular differentiation and wound healing potential of stem cells co-cultured with endothelial cells," *PloS one*, vol. 6, no. 1, p. e16114, 2011.

[21] J. Hur, C.-H. Yoon, H.-S. Kim, J.-H. Choi, H.-J. Kang, K.-K. Hwang, B.-H. Oh, M.-M. Lee, and Y.-

B. Park, "Characterization of two types of endothelial progenitor cells and their different contributions to neovasculogenesis.," *Arterioscler. Thromb. Vasc. Biol.*, vol. 24, no. 2, pp. 288–293, Feb. 2004.

[22] I. Ahrens, H. Domeij, D. Topcic, I. Haviv, R.-M. Merivirta, A. Agrotis, E. Leitner, J. B. Jowett, C. Bode, M. Lappas, and K. Peter, "Successful in vitro expansion and differentiation of cord blood derived CD34+ cells into early endothelial progenitor cells reveals highly differential gene expression.," *PloS one*, vol. 6, no. 8, p. e23210, 2011.

[23] J. M. Melero-Martin, M. E. De Obaldia, S.-Y. Kang, Z. A. Khan, L. Yuan, P. Oettgen, and J. Bischoff, "Engineering Robust and Functional Vascular Networks In Vivo With Human Adult and Cord Blood–Derived Progenitor Cells," *Circulation research*, vol. 103, no. 2, pp. 194–202, Jul. 2008.

[24] T. Walenda, S. Bork, P. Horn, F. Wein, R. Saffrich, A. Diehlmann, V. Eckstein, A. D. Ho, and W. Wagner, "Co-culture with mesenchymal stromal cells increases proliferation and maintenance of haematopoietic progenitor cells.," *J. Cell. Mol. Med.*, vol. 14, no. 1, pp. 337–350, Jan. 2010.

[25] A. Aguirre, J. A. Planell, and E. Engel, "Dynamics of bone marrow-derived endothelial progenitor cell/mesenchymal stem cell interaction in co-culture and its implications in angiogenesis," *Biochemical and biophysical research communications*, vol. 400, no. 2, pp. 284–291, Sep. 2010.

[26] M. B. Rookmaaker, M. C. Verhaar, C. J. M. Loomans, R. Verloop, E. Peters, P. E. Westerweel, T. Murohara, F. J. T. Staal, A. J. van Zonneveld, P. Koolwijk, T. J. Rabelink, and V. W. M. van Hinsbergh, "CD34+ cells home, proliferate, and participate in capillary formation, and in combination with CD34- cells enhance tube formation in a 3-dimensional matrix.," *Arterioscler. Thromb. Vasc. Biol.*, vol. 25, no. 9, pp. 1843–1850, Sep. 2005.

[27] J. M. Sorrell, M. A. Baber, and A. I. Caplan, "Influence of adult mesenchymal stem cells on in vitro vascular formation," *Tissue engineering. Part A*, vol. 15, no. 7, pp. 1751–1761, Jul. 2009.

[28] R. Maia, K. Beltrame, P. L. Granja, C. C. Barrias, and G. Rodrigues, *Self-assembly of MSC-ECM microtissues on soft hydrogel matrices*. *Submitted*, 2013

[29] M. W. Tibbitt and K. S. Anseth, "Hydrogels as extracellular matrix mimics for 3D cell culture.," *Biotechnol. Bioeng.*, vol. 103, no. 4, pp. 655–663, Jul. 2009.

[30] M. B. Evangelista, S. X. Hsiong, R. Fernandes, P. Sampaio, H.-J. Kong, C. C. Barrias, R. Salema, M. A. Barbosa, D. J. Mooney, and P. L. Granja, "Upregulation of bone cell differentiation through immobilization within a synthetic extracellular matrix.," *Biomaterials*, vol. 28, no. 25, pp. 3644–3655, Sep. 2007.

[31] S. J. Bidarra, C. C. Barrias, K. B. Fonseca, M. A. Barbosa, R. A. Soares, and P. L. Granja, "Injectable in situ crosslinkable RGD-modified alginate matrix for endothelial cells delivery," *Biomaterials*, vol. 32, no. 31, pp. 7897–7904, Nov. 2011.

[32] K. B. Fonseca, S. J. Bidarra, M. J. Oliveira, P. L. Granja, and C. C. Barrias, "Molecularly designed alginate hydrogels susceptible to local proteolysis as three-dimensional cellular microenvironments.," *Acta Biomater*, vol. 7, no. 4, pp. 1674–1682, Apr. 2011.

[33] E. A. Silva and D. J. Mooney, "Spatiotemporal control of vascular endothelial growth factor delivery from injectable hydrogels enhances angiogenesis," *Journal of thrombosis and haemostasis : JTH*, vol. 5, no. 3, pp. 590–598, Mar. 2007.

[34] S. M. Jay, B. R. Shepherd, J. P. Bertram, J. S. Pober, and W. M. Saltzman, "Engineering of multifunctional gels integrating highly efficient growth factor delivery with endothelial cell transplantation," *FASEB journal : official publication of the Federation of American Societies for Experimental Biology*, vol. 22, no. 8, pp. 2949–2956, Aug. 2008.

[35] A. M. Goodwin, "In vitro assays of angiogenesis for assessment of angiogenic and anti-angiogenic agents," *Microvascular research*, vol. 74, no. 2, pp. 172–183, Sep-Nov 2007.

[36] T. I. Valdes, D. Kreutzer, and F. Moussy, "The chick chorioallantoic membrane as a novel in vivo model for the testing of biomaterials," *Journal of biomedical materials research*, vol. 62, no. 2, pp. 273–282, Nov. 2002.

[37] X. Liu, X. Wang, A. Horii, X. Wang, L. Qiao, S. Zhang, and F. Z. Cui, "In vivo studies on angiogenic activity of two designer self-assembling peptide scaffold hydrogels in the chicken embryo chorioallantoic membrane," *Nanoscale*, vol. 4, no. 8, pp. 2720–2727, Apr. 2012.

[38] G. Finkenzeller, S. Graner, C. J. Kirkpatrick, S. Fuchs, and G. B. Stark, "Impaired in vivo vasculogenic potential of endothelial progenitor cells in comparison to human umbilical

vein endothelial cells in a spheroid-based implantation model.," *Cell Prolif.*, vol. 42, no. 4, pp. 498–505, Aug. 2009.

[39] T. Fietz, B. Reufi, C. Mucke, E. Thiel, and W. U. Knauf, "Flow cytometric CD34+ determination in stem cell transplantation: before or after cryopreservation of grafts?," *J Hematother Stem Cell Res*, vol. 11, no. 2, pp. 429–435, Apr. 2002.

[40] *CD markers handbook*. [Online]. Available: http://www.bdbiosciences.com/documents/cd_marker_handbook.pdf. [Accessed: 13-Sep-2013].

[41] H. Kim, H.-J. Cho, S.-W. Kim, B. Liu, Y. J. Choi, J. Lee, Y.-D. Sohn, M.-Y. Lee, M. A. Houge, and Y.-S. Yoon, "CD31+ cells represent highly angiogenic and vasculogenic cells in bone marrow: novel role of nonendothelial CD31+ cells in neovascularization and their therapeutic effects on ischemic vascular disease.," *Circulation research*, vol. 107, no. 5, pp. 602–614, Sep. 2010.

[42] S. Rafii and D. Lyden, "Therapeutic stem and progenitor cell transplantation for organ vascularization and regeneration.," *Nature medicine*, vol. 9, no. 6, pp. 702–712, Jun. 2003.

[43] A. Schmeisser, C. D. Garlichs, H. Zhang, S. Eskafi, C. Graffy, J. Ludwig, R. H. Strasser, and W. G. Daniel, "Monocytes coexpress endothelial and macrophagocytic lineage markers and form cord-like structures in Matrigel® under angiogenic conditions," *Cardiovascular research*, vol. 49, no. 3, pp. 671–680, Feb. 2001.

[44] J. Rehman, J. Li, C. M. Orschell, and K. L. March, "Peripheral blood 'endothelial progenitor cells' are derived from monocyte/macrophages and secrete angiogenic growth factors.," *Circulation*, vol. 107, no. 8, pp. 1164–1169, Mar. 2003.

[45] E. E. Robinson, R. A. Foty, and S. A. Corbett, "Fibronectin matrix assembly regulates alpha5beta1-mediated cell cohesion.," *Mol. Biol. Cell*, vol. 15, no. 3, pp. 973–981, Mar. 2004.

[46] R. R. Rao, A. W. Peterson, J. Ceccarelli, A. J. Putnam, and J. P. Stegemann, "Matrix composition regulates three-dimensional network formation by endothelial cells and mesenchymal stem cells in collagen/fibrin materials," *Angiogenesis*, vol. 15, no. 2, pp. 253–264, Jun. 2012.

[47] X. Zhou, R. G. Rowe, N. Hiraoka, J. P. George, D. Wirtz, D. F. Mosher, I. Virtanen, M. A. Chernousov, and S. J. Weiss, "Fibronectin fibrillogenesis regulates three-dimensional neovessel formation.," *Genes Dev.*, vol. 22, no. 9, pp. 1231–1243, May 2008.

[48] Y. C. Chen, R. Z. Lin, H. Qi, Y. Yang, H. Bae, J. M. Melero-Martin, and A. Khademhosseini, "Functional Human Vascular Network Generated in Photocrosslinkable Gelatin Methacrylate Hydrogels," *Advanced functional materials*, vol. 22, no. 10, pp. 2027–2039, May 2012.

[49] A. N. Stratman, K. M. Malotte, R. D. Mahan, M. J. Davis, and G. E. Davis, "Pericyte recruitment during vasculogenic tube assembly stimulates endothelial basement membrane matrix formation.," *Blood*, vol. 114, no. 24, pp. 5091–5101, Dec. 2009.

[50] J. J. Moon, J. E. Saik, R. A. Poché, J. E. Leslie-Barbick, S.-H. Lee, A. A. Smith, M. E. Dickinson, and J. L. West, "Biomimetic hydrogels with pro-angiogenic properties.," *Biomaterials*, vol. 31, no. 14, pp. 3840–3847, May 2010.

[51] N. Li, P. Feugier, B. Serrurrier, V. Latger-Cannard, J.-F. Lesesve, J.-F. Stoltz, and A. Eljaafari, "Human mesenchymal stem cells improve ex vivo expansion of adult human CD34+ peripheral blood progenitor cells and decrease their allostimulatory capacity.," *Exp. Hematol.*, vol. 35, no. 3, pp. 507–515, Mar. 2007.

[52] X. Lu, S. V. Baudouin, J. I. Gillespie, J. J. Anderson, and A. M. Dickinson, "A comparison of CFU-GM, BFU-E and endothelial progenitor cells using ex vivo expansion of selected cord blood CD133(+) and CD34(+) cells.," *Cytotherapy*, vol. 9, no. 3, pp. 292–300, 2007.

Supplementary Data

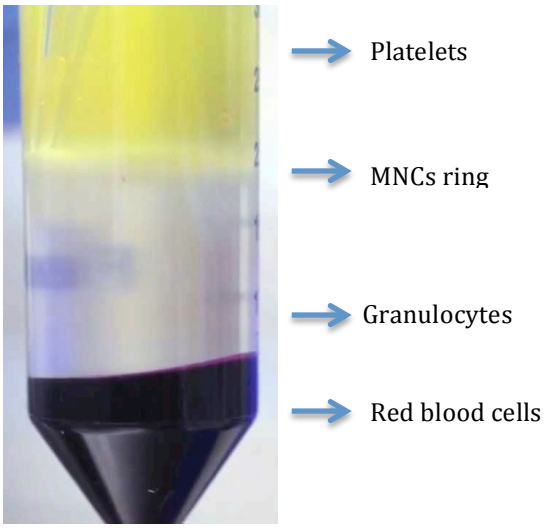

Figure S-1: Location of the ring formed by MNCs. *(Adapted from www.stemcell.com)*

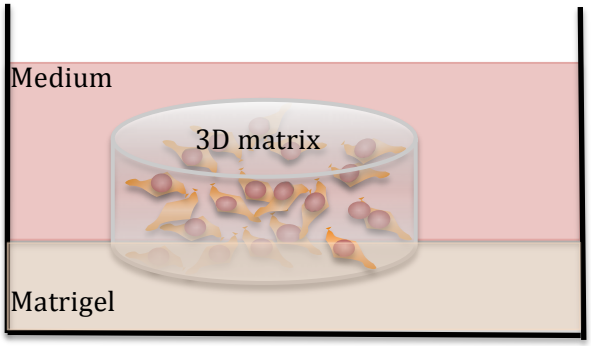

Figure S-2: Representation of a 3D culture migration assay.

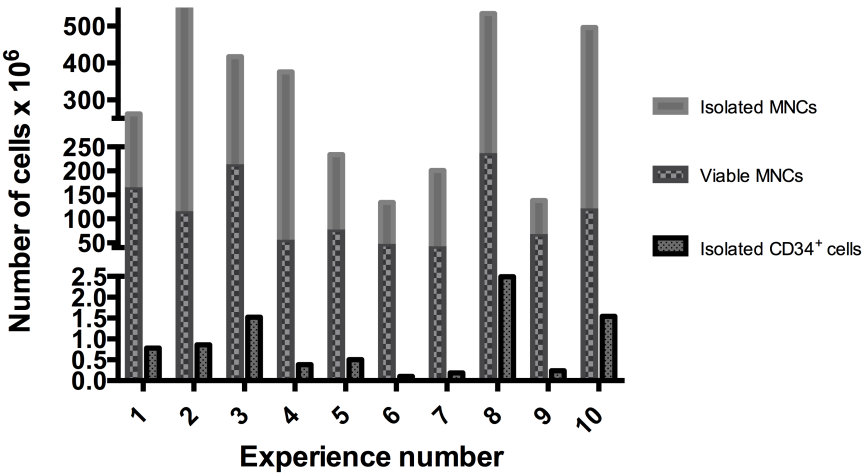

Figure S-3 - Number of cells isolated from each donor's blood. Isolated MNCs refers to the number of MNCs isolated from the blood; Viable MNCs are the ones that remain viable after defrosting and isolated CD34+ cells are the ones that result from isolation in MACS columns.

Table S-III – FACS analysis of CD34, CD31 and CD38 expression in each sample. Each experiment derived from a different umbilical cord blood sample. Values are expressed in percentage of the overall gated population (live cells). Negative 1 and Negative 2 are the flow through suspensions from the first and second MACS columns, respectively. Positive is the flow through from the second column, outside the magnetic field – CD34 positively marked cells.

		EXP. 6	EXP. 8	EXP. 9	EXP. 10	Average	Std. Dev.
Negative 1	% viable cells	60.40	92.00	79.80	67.50	74.93	12.06
	% CD34+ cells	1.28	0.12	0.42	0.03	0.46	0.49
	% CD31+ cells	60.68	85.02	85.41	81.86	78.24	10.23
	% CD34+CD38- cells	0.00	0.00	0.00	0.00	0.00	0.00
	% CD34+CD31+ cells	4.25	15.06	20.66	25.89	16.46	8.03
Negative 2	% viable cells	75.30	77.00	77.40	75.50	76.30	0.91
	% CD34+ cells	25.56	6.13	0.08	2.95	8.68	9.98
	% CD31+ cells	73.95	85.37	83.54	86.10	82.24	4.88
	% CD34+CD38- cells	2.15	0.60	0.47	0.00	0.81	0.93
	% CD34+CD31+ cells	43.70	25.85	24.36	8.81	25.68	12.36
Positive	% viable cells	87.20	62.30	82.80	42.60	68.73	17.77
	% CD34+ cells	98.29	94.58	60.42	86.60	84.97	14.79
	% CD31+ cells	98.69	98.43	94.88	99.26	97.81	1.72
	% CD34+CD38- cells	6.52	0.64	21.46	49.71	19.58	18.98
	% CD34+CD31+ cells	98.49	96.23	76.59	93.61	91.23	8.63

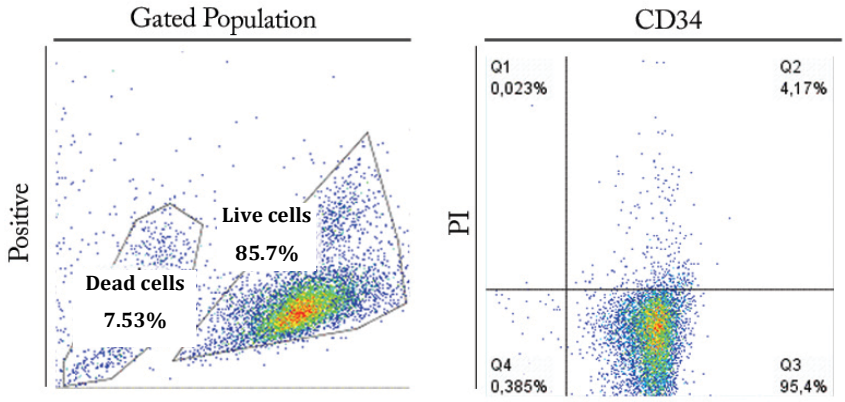

Figure S-4 - FACS scatter images of cells marked with PI. The first image represents the positive sample's gated population (FSC-H vs. SSC-H), with the distinction between live and dead cells. The second image displays the scatter for expression of CD34 (FL1-H) versus PI (FL3-H) within the live cells population. Here we can see that within this gate there are almost no dead cells (no expression of PI) and that their majority expresses CD34.

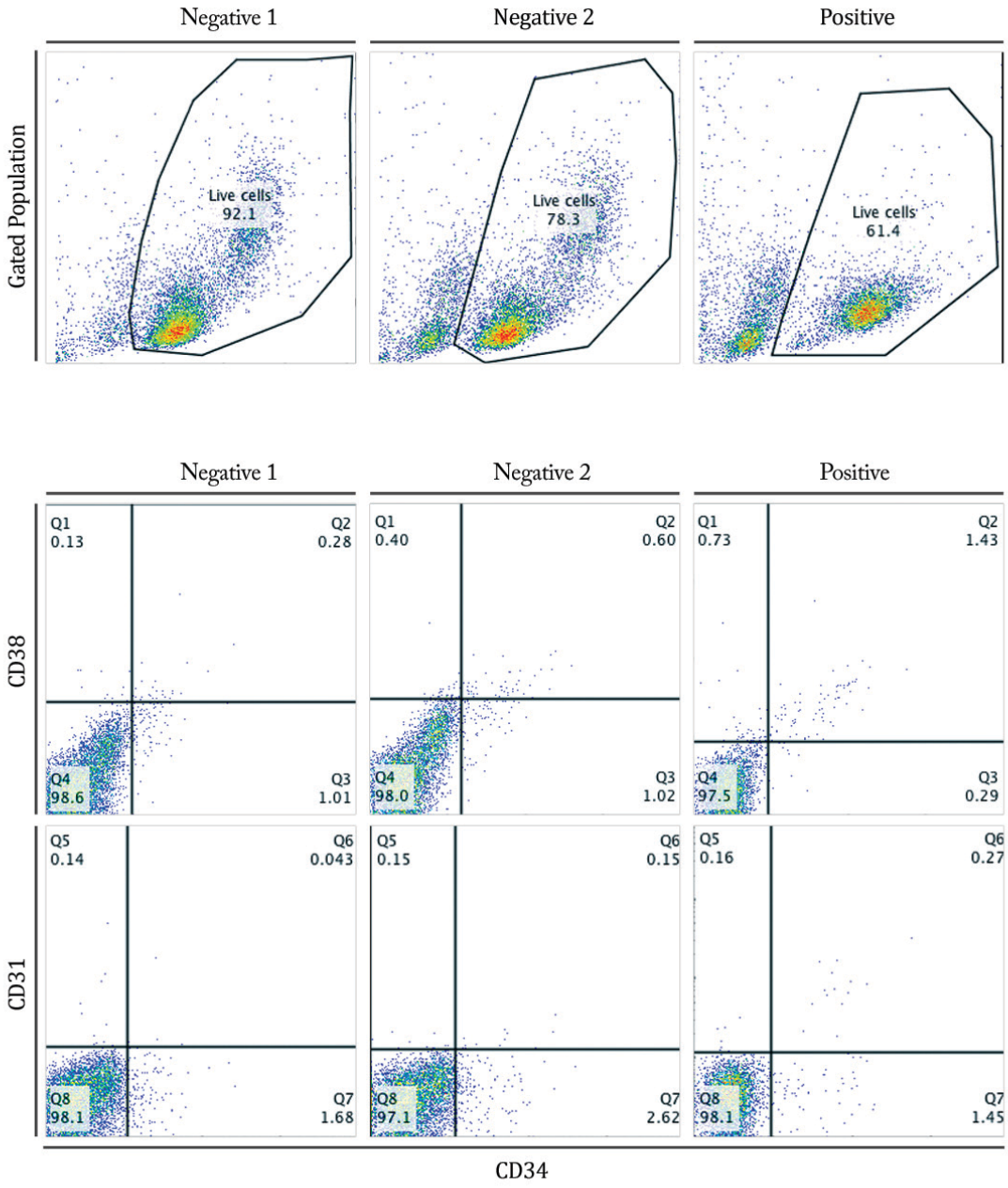

Figure S-5 - FACS scatter images of isotype. The first three images represent each sample's gated population (FSC-H vs. SSC-H). The second row displays the scatters for expression of CD34 (FL1-H) versus CD38 (FL2-H) and the last row has the scatters for CD34 versus CD31 (FL4-H). These are images from EXP.8, but are representative of the four experiments that were analyzed.

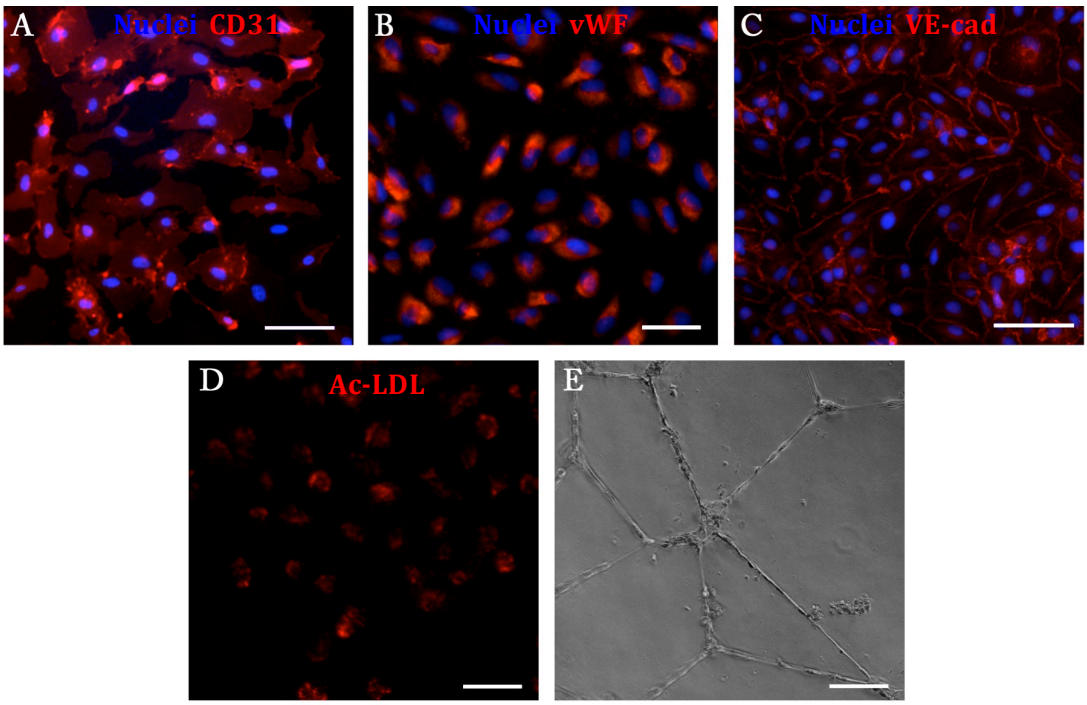

Figure S-6 – Analysis of protein expression in HUVECs using immunohistochemistry. A, B, C) Immunofluorescence protein expression results: CD31, vWF and VE-cadherin (Scale bar = 100, 50 and 100 µm); E) Ac-LDL uptake (Scale bar = 50 µm); F) Phase contrast photomicrograph of differentiated cells cultured in Matrigel for 24h (Scale bar = 150 µm).

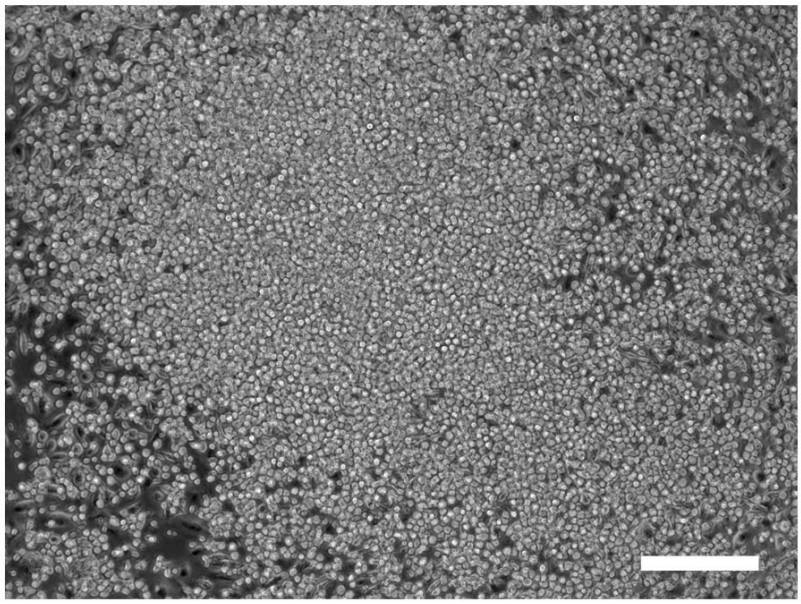

Figure S-7 – Morphology of CD34^{+}-derived cells, 21 days after plating. Big agglomerates of round cells were formed. Scale bar = 200 µm.

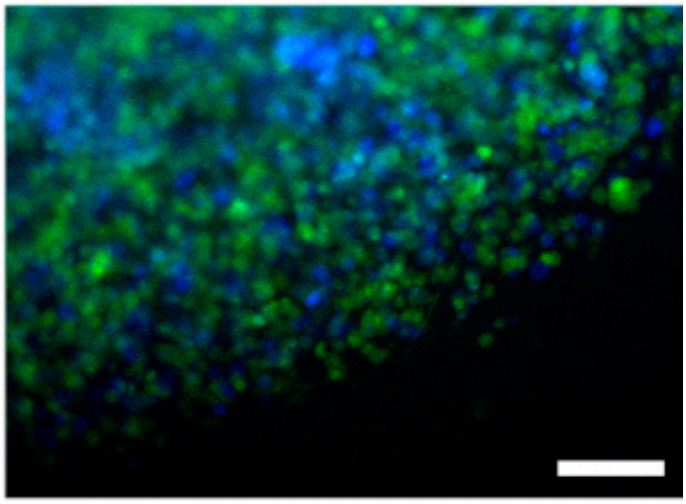

Figure S-8 – HUVECs were efficiently stained with CellTracker Green and MSCs with CellTracker Blue. No double staining was detected in separated channels, although only the periphery of the disk could be focused. *Sample was visualized under inverted fluorescence microscope. Scale bar=150 µm.*